Technische Universität Berlin
Institut für Mathematik

Systematic discretization of input-output maps of linear infinite dimensional systems

(Completely revised version of Preprint 2006-06)

Michael Schmidt

Preprint 2008-29

Preprint-Reihe des Instituts für Mathematik
Technische Universität Berlin

Report 2008-29 **August 2008**

SYSTEMATIC DISCRETIZATION OF INPUT-OUTPUT MAPS OF LINEAR INFINITE-DIMENSIONAL SYSTEMS

MICHAEL SCHMIDT*

Abstract. Many model reduction techniques take a semi-discretization of a PDE model as starting point and aim then at an accurate approximation of its input/output map. In this contribution, we discuss the direct discretization of the i/o map of the infinite-dimensional system for a general class of linear time-invariant systems with distributed inputs and outputs.

First, the input and output signals are discretized in space and time, resulting in the matrix representation of an approximated i/o-map. In a generalized sense, the matrix contains the Markov parameters of a corresponding time-discrete multi-input-multi-output system. Second, the system dynamics is approximated in form of the underlying evolution operator, in order to calculate the matrix representation numerically. The discretization framework, corresponding error estimates, a SVD-based system reduction method and a numerical application in an optimization problem are presented, and illustrated for a heat control system.

Key words. input-output map, discretization, infinite-dimensional control system, time-discrete MIMO system, model reduction, optimization, feedback control

AMS subject classifications. 39C20, 35B37

1. Introduction.

1.1. Motivation. The control of complex physical systems is a big challenge in many engineering applications as well as in mathematical research. Frequently, these control systems are modeled by infinite-dimensional state space systems on the basis of (instationary and nonlinear) partial differential equations (PDEs). On the one hand, space-discretizations resolving most of the state information typically lead to very large semi-discrete systems, on the other hand, popular design techniques for real-time controllers like robust control require linear models of very moderate size [13, 39].

Numerous approaches to bridge this gap are proposed in the literature, see e.g. [3, 12, 28] and the references therein. In some applications one is interested in low-order models capturing essential state dynamics. Then e.g. low-order modeling on the basis of physical insight [27, 36, 40] and models reduced by means of mathematical methods like Proper Orthogonal Decomposition (POD) [14] can be very useful. In this paper we focus on the frequent situation that models merely describing accurately the system's *input/output (i/o) map* are sufficient to realize efficient controls. Empirical or simulation-based black-box system identification [7, 30], and mathematical model reduction techniques like balanced truncation [28], moment matching [26] and recent variants of POD [42, 48] are tools to extract appropriate models.

Empirically and physically motivated approaches usually lack analytical estimates for the accuracy of the i/o map, for some mathematical model reduction techniques like balanced truncation such estimates exist. Most mathematical methods take, however, the space-discretized PDE as starting point, some of them even a time-invariant linearization. The preceding PDE space discretizations are often neglected by assuming that they are 'sufficiently accurate'. Thereby, the PDE discretizations rarely take the efficient approximation of the i/o map into account. On the one hand,

*Technische Universität Berlin, Institute of Mathematics, 10623 Berlin, Germany (mschmidt@math.tu-berlin.de), supported by DFG-Sonderforschungsbereich 557 'Control of complex turbulent shear flows'.

the state space discretization typically aims at a reduction of the global state space error and is thus still oriented at a *state simulation problem*. On the other hand, the i/o error due to the discretization of spatially distributed inputs and outputs is rarely considered rigorously. Aiming at a low-dimensional model of the i/o behavior in the end, starting with a space-discretization of the original state space model can be considered as a conceptual detour.

1.2. An integral approach to derive i/o models with error estimates. In this paper we investigate a new and integral approach to derive low-order models with error estimates for the i/o behavior. We focus directly on the i/o map of the *original* infinite-dimensional system, in the following denoted by

$$\mathbb{G} : \mathcal{U} \to \mathcal{Y}, \qquad u = u(t,\theta) \mapsto y = y(t,\xi),$$

and suggest the following framework for its direct discretization for a general class of *linear time-invariant* systems (introduced in Section 2). Here u and y are input and output signals from Hilbert spaces $\mathcal{U}$ and $\mathcal{Y}$, respectively, which may vary in time t and space $\theta \in \Theta$ and $\xi \in \Xi$, with appropriate spatial domains Θ and Ξ. The framework consists of two steps.

1. *Approximation of signals (cf. Section 3).* We choose finite-dimensional subspaces $\bar{\mathcal{U}} \subset \mathcal{U}$ and $\bar{\mathcal{Y}} \subset \mathcal{Y}$ with bases $\{u_1, \ldots, u_{\bar{p}}\} \subset \bar{\mathcal{U}}$ and $\{y_1, \ldots, y_{\bar{q}}\} \subset \bar{\mathcal{Y}}$, and denote the corresponding orthogonal projections by $\mathbb{P}_{\bar{\mathcal{U}}}$ and $\mathbb{P}_{\bar{\mathcal{Y}}}$, respectively. Then, the approximation
$$\mathbb{G}_S = \mathbb{P}_{\bar{\mathcal{Y}}} \mathbb{G} \mathbb{P}_{\bar{\mathcal{U}}}$$
has a matrix representation $\mathbf{G} \in \mathbb{R}^{\bar{q} \times \bar{p}}$, for instance with elements $\mathbf{G}_{ij} = (y_i, \mathbb{G}u_j)_{\mathcal{Y}}$ if orthonormal bases are chosen in $\bar{\mathcal{U}}$ and $\bar{\mathcal{Y}}$.
2. *Approximation of system dynamics (cf. Section 4).* Frequently, $\mathbb{G}$ arises from a linear PDE state space model. Then the components $\mathbf{G}_{ij} = (y_i, \mathbb{G}u_j)_{\mathcal{Y}}$ can be approximated by *numerically simulating* the state space model successively for inputs u_j, $j = 1, \ldots, \bar{p}$ and by testing the resulting outputs against all $y_1, \ldots, y_{\bar{q}}$. The result is an approximation $\mathbb{G}_{DS}$ of $\mathbb{G}_S$. Considering time-invariant systems and choosing basis functions with a space-time tensor structure, like
$$u_{i(j,l)}(t;\theta) = \phi_j(t)\mu_l(\theta), \quad y_{j(i,k)}(t;\xi) = \psi_i(t)\nu_k(\xi),$$
this task reduces to the approximation of observations $(\nu_k, Cz_l(t))_Y$, with states $z_l(t) = S(t)B\mu_l$. Here $S(t)$, B and C are the system's evolution semigroup, input and output operator, respectively. Hence, $Cz_l(t)$ can be considered as the system's impulse response corresponding to an initial value μ_l, and $z_l(t)$ can be approximated by numerically solving a homogeneous PDE.

We discuss some prospects of this framework.

Error estimation (cf. Section 5). The total error ϵ_{DS} can be estimated by the *signal* approximation error ϵ_S and the *dynamical* approximation error ϵ_D, i.e.

$$\underbrace{\|\mathbb{G} - \mathbb{G}_{DS}\|}_{=:\epsilon_{DS}} \leq \underbrace{\|\mathbb{G} - \mathbb{G}_S\|}_{=:\epsilon_S} + \underbrace{\|\mathbb{G}_S - \mathbb{G}_{DS}\|}_{=:\epsilon_D}, \tag{1.1}$$

where the norms still have to be specified. As main result of this paper, Thm. 5.1 shows how to choose $\bar{\mathcal{U}}$ and $\bar{\mathcal{Y}}$ in the first step and the accuracy tolerances for the numerical solutions of the underlying PDEs in the second step such that ϵ_S and ϵ_D balance and that $\epsilon_S + \epsilon_D < \texttt{tol}$ for a given tolerance `tol`.

Progressive reduction of the signal error. Choosing hierarchical bases in $\bar{\mathcal{U}}$ and $\bar{\mathcal{Y}}$, the error ϵ_S can be progressively reduced by adding further basis functions $u_{\bar{p}+1}, u_{\bar{p}+2}, \ldots$ and $y_{\bar{q}+1}, y_{\bar{q}+2}, \ldots$ resulting in additional columns and rows of the matrix representation.

Matrix reduction via multilinear SVDs (cf. Section 6). The matrix representation of $\mathbb{G}_{DS}$ allows for low rank approximations with error estimates on the basis of so-called higher order singular value decompositions (HOSVDs) [19], respecting the time-space tensor structure of the basis functions. The corresponding singular vectors represent the most relevant input and output signals.

Actuators and sensors for distributed inputs and outputs. Thinking of practical applications, input signals $u(t;\theta)$ and output signals $y(t;\xi)$ are often generated and measured by actuators and sensors with limited spatial and temporal resolutions, such that 'realizable' input and output signals naturally belong to finite dimensional subspaces $\bar{\mathcal{U}}$ and $\bar{\mathcal{Y}}$, respectively. Error estimates of the form (1.1) and the extraction of relevant input and output signals on the basis of HOSVDs may thus provide useful information for efficient sensor and actuator design, see Section 6. Note that classical approaches (where the control system is first discretized in space and then model reduction is applied) rarely take the error due to input and output space-discretizations into account.

Control Design (cf. Section 6). The matrix representation $\mathbf{G} = [\mathbf{G}_{ij}]$ may directly be used in control design, or a state realization of the i/o model $\mathbb{G}_{DS}$ can be used as basis for many classical control design algorithms.

1.3. Relation to numerical analysis, control theory and optimal control. From the point of view of numerical analysis, the presented approach is a Galerkin approximation of the i/o map, which is a Volterra integral operator arising from the semigroup representation of the evolution system. The corresponding error estimates are based on standard interpolation theory in Sobolev spaces and on error results for the numerical solution of evolution equations.

From the point of view of control theory, the linear time-continuous infinite-dimensional system with distributed controls and observations is first approximated by a time-discrete multi-input-multi-output system, the corresponding Markov parameters are then approximated by numerically calculating impulse responses.

Using the approximated i/o map in optimal control applications corresponds to a pronounced form of the concept 'first discretize, then optimize' since the original system is discretized in space *and* time. On the one hand, this entails the risk of loosing essential structural features of the original control problem, which may lead e.g. to instabilities or simply failing of the calculated controls. The analytical investigation of the behavior of the approximated i/o map in control applications is an important future task. On the other hand, the algebraic representation of the i/o-map enables the use of very fast methods for model reduction and control design, and the error results for the full discretization may help to take effects of digitizing inputs and outputs for processing by discrete controllers into account.

Finally, we aim to mention some other approaches which directly focus on the original infinite-dimensional system or control problem. Balanced Truncation and POD have been formulated in infinite-dimensional function spaces, see e.g. [14, 18, 43]. In sophisticated simulations and optimal control applications, state and control discretization errors and even modeling errors are adaptively controlled with respect to their effect on quantities of interest, see e.g. [11, 15].

1.4. Notation. For $\Omega \subset \mathbb{R}^d$, $d \in \mathbb{N}$, $L^2(\Omega)$ denotes the usual Lebesgue space of square-integrable functions, and $H^\alpha(\Omega)$, $\alpha \in \mathbb{N}_0$ denotes the corresponding Sobolev spaces of α-times weakly differentiable functions. We interpret functions v, which vary in space and time, optionally as classical functions $v : [0,T] \times \Omega \to \mathbb{R}$ with values $v(t;x) \in \mathbb{R}$, or as *abstract* functions $v : [0,T] \to \mathbb{R}$ with values in a function space X such as $X = H^\alpha(\Omega)$. Correspondingly, $H^\alpha(0,T;H^\beta(\Omega))$, with $\alpha, \beta \in \mathbb{N}_0$, denotes the space of equivalence classes of functions $v : [0,T] \to H^\beta(\Omega)$ with $t \mapsto \|v\|_{H^\beta(\Omega)}$ being α-times weakly differentiable, for details see e.g. [22]. We introduce Hilbert spaces

$$\begin{aligned}
H^{\alpha,\beta}((0,T)\times\Omega) &:= H^\alpha(0,T;L^2(\Omega)) \cap L^2(0,T;H^\beta(\Omega)), \\
\|v\|_{H^{\alpha,\beta}((0,T)\times\Omega)} &:= \|v\|_{H^\alpha(0,T;L^2(\Omega))} + \|v\|_{L^2(0,T;H^\beta(\Omega))},
\end{aligned}$$

see e.g. [37]. By $C([0,T];X)$ and $C^\alpha([0,T];X)$ we denote the space of functions $v : [0,T] \to X$ which are continuous respectively α-times continuously differentiable. For two normed spaces X and Y, $\mathscr{L}(X,Y)$ denotes the set of bounded linear operators $X \to Y$, and we abbreviate $\mathscr{L}(X) := \mathscr{L}(X,X)$. For $\alpha \in \mathbb{N}$, $L^\alpha(0,T;\mathscr{L}(X,Y))$ denotes the space of operator-valued functions $K : [0,T] \to \mathscr{L}(X,Y)$ with $t \mapsto \|K(t)\|_{\mathscr{L}(X,Y)} = \sup_{x\neq 0} \|K(t)x\|_Y / \|x\|_X$ lying in $L^\alpha(0,T)$. Vectors, often representing a discretization of a function v, are written in corresponding small bold letters $\mathbf{v}$, whereas matrices, often representing a discrete version of an operator like $\mathbb{G}$ or G, are written in bold capital letters $\mathbf{G}$. $\mathbb{R}^{\alpha\times\beta}$ stands for the set of real $\alpha \times \beta$ matrices, and $\mathbf{A} \otimes \mathbf{B}$ denotes the Kronecker tensor product of two matrices $\mathbf{A}$ and $\mathbf{B}$.

2. I/o maps of ∞-dimensional LTI state space systems. We consider infinite-dimensional linear time-invariant systems of first order

$$\partial_t z(t) = Az(t) + Bu(t), \quad t \in (0,T], \tag{2.1a}$$

$$z(0) = z^0, \tag{2.1b}$$

$$y(t) = Cz(t), \quad t \in [0,T]. \tag{2.1c}$$

Here for every time $t \in [0,T]$, the state $z(t)$ is supposed to belong to a Hilbert space Z like $Z = L^2(\Omega)$, where Ω is a subset of $\mathbb{R}^{d_\Omega}$ with $d_\Omega \in \mathbb{N}$. A is a densely defined unbounded operator $A : Z \supset D(A) \to Z$, generating a C^0-semigroup $(S(t))_{t\geq 0}$ on Z. The control operator B belongs to $\mathscr{L}(U,Z)$ and the observation operator C to $\mathscr{L}(Z,Y)$, where $U = L^2(\Theta)$ and $Y = L^2(\Xi)$ with subsets $\Theta \subset \mathbb{R}^{d_1}$ and $\Xi \subset \mathbb{R}^{d_2}$, $d_1, d_2 \in \mathbb{N}$.

We recall how a linear bounded i/o-map $\mathbb{G} \in \mathscr{L}(\mathcal{U},\mathcal{Y})$ with

$$\mathcal{U} = L^2(0,T;U) \quad \text{and} \quad \mathcal{Y} = L^2(0,T;Y)$$

can be associated to (2.1), for details see e.g. [41, Ch. 4]. It is well-known that for initial values $z_0 \in D(A)$ and controls $u \in C^1([0,T];Z)$, a unique *classical solution* $z \in C([0,T];Z) \cap C^1((0,T);Z)$ of (2.1) exists. For $z_0 \in Z$ and $u \in \mathcal{U}$, the well-defined function

$$z(t) = S(t)z_0 + \int_0^t S(t-s)Bu(s)\,ds, \quad t \in [0,T], \tag{2.2}$$

is called a *mild solution* of (2.1). A mild solution of (2.1) is unique, belongs to $C([0,T];Z)$ and is the uniform limit of classical solutions [41]. Hence, the output signal $y(t) = Cz(t)$ is well-defined and belongs to $\mathcal{Y} \cap C([0,T];Y)$. In particular, the ouput signals $y(u) \in \mathcal{Y}$ arising from input signals $u \in \mathcal{U}$ and zero initial conditions $z_0 \equiv 0$ allow to define the linear i/o-map $\mathbb{G} : \mathcal{U} \to \mathcal{Y}$ of the system (2.1) by $u \mapsto y(u)$. It is possible to represent $\mathbb{G}$ as a convolution with the kernel function $K \in L^2(-T,T;\mathscr{L}(U,Y))$,

$$K(t) = \begin{cases} CS(t)B, & t \geq 0 \\ 0, & t < 0 \end{cases}. \tag{2.3}$$

LEMMA 2.1. *The i/o-map $\mathbb{G}$ of (2.1) has the representation*

$$(\mathbb{G}u)(t) = \int_0^T K(t-s)u(s)\,ds, \quad t \in [0,T], \tag{2.4}$$

belongs to $\mathscr{L}(\mathcal{U},\mathcal{Y}) \cap \mathscr{L}(\mathcal{U}, C([0,T],\mathcal{Y}))$ and satisfies

$$\|\mathbb{G}\|_{\mathscr{L}(\mathcal{U},\mathcal{Y})} \leq \sqrt{T}\|K\|_{L^2(0,T;\mathscr{L}(U,Y))}. \tag{2.5}$$

Proof. Since C is bounded, the representation of $y = Cz$ based on (2.2) can be reformulated as in (2.4), see e.g. [22] for the theory of Bochner integrals. For general $K \in L^2(-T,T;\mathscr{L}(U,Y))$, a generalized Hölder's inequality yields that for fixed $t \in [0,T]$, the function $s \to K(t-s)u(s)$ belongs to $L^1(0,T;\mathscr{L}(U,Y))$ with

$$\|(\mathbb{G}u)(t)\|_Y \leq \|u\|_{\mathcal{U}}\|K(t-\cdot)\|_{L^2(0,T;\mathscr{L}(U,Y)},$$

and by integrating over $[0,T]$ we obtain (2.5). □

REMARK 1. *The i/o-map $\mathbb{G}$ is* causal *in the sense that $y(t)$ only depends on $u_{|[0,t)}$ for all $t \in [0,T]$, and $\mathbb{G}$ is* time-invariant *in the sense that if $y = \mathbb{G}u$ then $\sigma_\tau y = \mathbb{G}(\sigma_\tau u)$ for all $\tau \in [0,T]$. Here σ_τ is a shift operator with $(\sigma_\tau u)(t) = u(t-\tau)$ for $t \in [\tau,T]$ and $(\sigma_\tau u)(t) = 0$ for $t \in [0,\tau)$.*

EXAMPLE 1. *As prototype for a parabolic system, we consider the heat equation with homogeneous Dirichlet boundary conditions and assume that Ω has a C^2-boundary. In this case, $Z = L^2(\Omega)$ and the operator A in (2.1) coincides with the Laplace operator*

$$A = \triangle : D(A) = H^2(\Omega) \cap H_0^1(\Omega) \subset Z \to Z. \tag{2.6}$$

Since A is the infinitesimal generator of an analytic C^0-semigroup of contractions $(S(t))_{t\geq 0}$, the mild solution z of (2.1) exhibits the following stability and regularity properties, see e.g. [41, Ch. 7] and [25].

(i) If $z_0 = 0$ and $u \in \mathcal{U}$, then $z \in H^{1,2}((0,T) \times \Omega)$ with

$$\|z\|_{H^{1,2}((0,T)\times\Omega)} \leq c\|u\|_{\mathcal{U}}. \tag{2.7}$$

(ii) Assume that $u \equiv 0$. For $z_0 \in D(A)$ we have $z \in C^1([0,T];D(A))$, but for $z_0 \in Z$ we only have $z \in C^1((0,T];D(A))$.

We will consider concrete choices of Ω, B and C in Section 6. We note that if the observation preserves the inherent state regularity in the sense that

$$C_{|H^2(\Omega)} \in \mathscr{L}(H^2(\Omega), H^2(\Xi)), \tag{2.8}$$

then $\mathbb{G} \in \mathscr{L}(\mathcal{U}, \mathcal{Y}_s)$ *and also*

$$\mathbb{G}_{|\mathcal{U}_s} \in \mathscr{L}(\mathcal{U}_s, \mathcal{Y}_s), \quad \text{with } \mathcal{U}_s = H^{1,2}((0,T) \times \Theta), \quad \mathcal{Y}_s = H^{1,2}((0,T) \times \Xi). \tag{2.9}$$

In fact, for $u \in \mathcal{U}_s$*, we have* $\|u\|_{\mathcal{U}} \leq \|u\|_{\mathcal{U}_s}$*, and for* $u \in \mathcal{U}$*, we have* $\|\mathbb{G}u\|_{\mathcal{Y}_s} \leq c'\|z\|_{H^{1,2}((0,T)\times\Omega)} \leq c\,c'\|u\|_{\mathcal{U}}$*, where* $c' = \max\{\|C\|_{\mathscr{L}(L^2(\Omega),L^2(\Xi))}, \|C\|_{\mathscr{L}(H^2(\Omega),H^2(\Xi))}\}$ *and* c *is the constant in* (2.7).

Remark 2. *Many other linear time-invariant systems with distributed controls and observations admit a representation of the i/o map via* (2.4) *and exhibit properties similar to* (2.9)*. This is, for instance, the case for the heat equation with homogeneous Neumann boundary conditions, and also for more general parabolic equations, see [37] and [38]. For Stokes systems, results similar to* (2.4) *and* (2.9) *are obtained by working with appropriate subspaces of divergence-free functions, see [44]. Wave equations with second order time derivatives can be represented in form of* (2.1) *and* (2.4) *by means of an order reduction. Though hyperbolic systems do not have the smoothing property of parabolic systems, they preserve the regularity of the data and results similar to* (2.9) *can be obtained due to the restriction to input signals of higher regularity in time, see [37, p. 95]. Note, however, that systems with boundary control or pointwise observation do not fit directly into the setting* (2.1).

3. Discretization of signals.

3.1. Space-time discretization and matrix representation. In order to discretize the input signals $u \in \mathcal{U}$ and $y \in \mathcal{Y}$ in space and time, we choose four families $\{U_{h_1}\}_{h_1>0}$, $\{Y_{h_2}\}_{h_2>0}$, $\{\mathcal{R}_{\tau_1}\}_{\tau_1>0}$ and $\{\mathcal{S}_{\tau_2}\}_{\tau_2>0}$ of subspaces $U_{h_1} \subset U$, $Y_{h_2} \subset Y$, $\mathcal{R}_{\tau_1} \subset L^2(0,T)$ and $\mathcal{S}_{\tau_2} \subset L^2(0,T)$ of finite dimensions $p(h_1) = dim(U_{h_1})$, $q(h_2) = dim(Y_{h_2})$, $r(\tau_1) = dim(\mathcal{R}_{\tau_1})$ and $s(\tau_2) = dim(\mathcal{S}_{\tau_2})$. We then define

$$\begin{aligned}
\mathcal{U}_{h_1,\tau_1} &= \{u \in \mathcal{U} : \, u(t;\cdot) \in U_{h_1}, \, u(\cdot;\theta) \in \mathcal{R}_{\tau_1} \quad \text{for almost every } \, t \in [0,T], \theta \in \Theta\},\\
\mathcal{Y}_{h_2,\tau_2} &= \{y \in \mathcal{Y} : \, y(t;\cdot) \in Y_{h_2}, \, y(\cdot;\xi) \in \mathcal{S}_{\tau_2} \quad \text{for almost every } \, t \in [0,T], \xi \in \Xi\}.
\end{aligned}$$

We denote the orthogonal projections onto these subspaces by $\mathbb{P}_{\mathcal{U},h_1,\tau_1} \in \mathscr{L}(\mathcal{U})$ and $\mathbb{P}_{\mathcal{Y},h_2,\tau_2} \in \mathscr{L}(\mathcal{Y})$. As first step of the approximation of $\mathbb{G}$, we define

$$\mathbb{G}_S = \mathbb{G}_S(h_1,\tau_1,h_2,\tau_2) = \mathbb{P}_{\mathcal{Y},h_2,\tau_2}\mathbb{G}\mathbb{P}_{\mathcal{U},h_1,\tau_1} \in \mathscr{L}(\mathcal{U},\mathcal{Y}). \tag{3.1}$$

In order to obtain a matrix representation of $\mathbb{G}_S$, we introduce families of bases $\{\mu_1, \dots, \mu_p\}$ of U_{h_1}, $\{\nu_1, \dots, \nu_q\}$ of Y_{h_2}, $\{\phi_1, \dots, \phi_r\}$ of $\mathcal{R}_{\tau_1}$ and $\{\psi_1, \dots, \psi_s\}$ of $\mathcal{S}_{\tau_2}$ and corresponding mass matrices $\mathbf{M}_{U,h_1} \in \mathbb{R}^{p\times p}$, $\mathbf{M}_{Y,h_2} \in \mathbb{R}^{q\times q}$, $\mathbf{M}_{\mathcal{R},\tau_1} \in \mathbb{R}^{r\times r}$ and $\mathbf{M}_{\mathcal{S},\tau_2} \in \mathbb{R}^{s\times s}$, for instance via

$$[\mathbf{M}_{U,h_1}]_{ij} = (\mu_j, \mu_i)_U, \qquad i,j = 1,\dots,p.$$

These mass matrices induce, for instance via

$$(\mathbf{v},\mathbf{w})_{p;w} = \mathbf{v}^T\mathbf{M}_{U,h_1}\mathbf{w} \quad \text{for all } \mathbf{v},\mathbf{w} \in \mathbb{R}^p,$$

weighted scalar products and corresponding norms in the respective spaces, which we indicate by a subscript w, like $\mathbb{R}^p_w$ with $(\cdot,\cdot)_{p;w}$ and $\|\cdot\|_{p;w}$, in contrast to the canonical spaces like $\mathbb{R}^p$ with $(\cdot,\cdot)_p$ and $\|\cdot\|_p$. We represent signals $u \in \mathcal{U}_{h_1,\tau_1}$ and $y \in \mathcal{Y}_{h_2,\tau_2}$ as

$$u(t;\theta) = \sum_{k=1}^{p}\sum_{i=1}^{r}\mathbf{u}_i^k\phi_i(t)\mu_k(\theta), \qquad y(t;\xi) = \sum_{l=1}^{q}\sum_{j=1}^{s}\mathbf{y}_j^l\psi_j(t)\nu_k(\xi),$$

where $\mathbf{u}_i^k$ are the elements of a block-structured vector $\mathbf{u} \in \mathbb{R}^{pr}$ with p blocks $\mathbf{u}^k \in \mathbb{R}^r$, and the vector $\mathbf{y} \in \mathbb{R}^{qs}$ is defined similarly. Then

$$\|u\|_{\mathcal{U}} = \|\mathbf{u}\|_{pr;w}, \quad \text{and} \quad \|y\|_{\mathcal{Y}} = \|\mathbf{y}\|_{qs;w},$$

where $\|\cdot\|_{pr;w}$ and $\|\cdot\|_{qs;w}$ denote the weighted norms with respect to the mass matrices

$$\mathbf{M}_{\mathcal{U},h_1,\tau_1} = \mathbf{M}_{U,h_1} \otimes \mathbf{M}_{\mathcal{R},\tau_1} \in \mathbb{R}^{pr\times pr}, \quad \mathbf{M}_{\mathcal{Y},h_2,\tau_2} = \mathbf{M}_{Y,h_2} \otimes \mathbf{M}_{\mathcal{S},\tau_2} \in \mathbb{R}^{qs\times qs},$$

i.e. the corresponding coordinate isomorphisms $\kappa_{\mathcal{U},h_1,\tau_1} \in \mathscr{L}(\mathcal{U}_{h_1,\tau_1}, \mathbb{R}^{pr}_w)$ and $\kappa_{\mathcal{Y},h_2,\tau_2} \in \mathscr{L}(\mathcal{Y}_{h_2,\tau_2}, \mathbb{R}^{qs}_w)$ are unitary.

Finally, we obtain a matrix representation $\mathbf{G}$ of $\mathbb{G}_S$ by setting

$$\mathbf{G} = \mathbf{G}(h_1,\tau_1,h_2,\tau_2) = \kappa_{\mathcal{Y}}\mathbb{P}_{\mathcal{Y}}\mathbb{G}\mathbb{P}_{\mathcal{U}}\kappa_{\mathcal{U}}^{-1} \in \mathbb{R}^{qs\times pr}, \tag{3.2}$$

where the dependencies on h_1, τ_1, h_2, τ_2 have been partially omitted. Considering

$$\mathbf{H} = \mathbf{H}(h_1,\tau_1,h_2,\tau_2) := \mathbf{M}_{\mathcal{Y},h_2,\tau_2}\mathbf{G} \in \mathbb{R}^{qs\times pr}$$

as a block-structured matrix with $q\times p$ blocks $\mathbf{H}^{kl} \in \mathbb{R}^{s\times r}$ and block elements $\mathbf{H}^{kl}_{ij} \in \mathbb{R}$, we obtain the element-wise representation

$$\mathbf{H}^{kl}_{ij} = [\mathbf{M}_{\mathcal{Y}}\kappa_{\mathcal{Y}}\mathbb{P}_{\mathcal{Y}}\mathbb{G}(\mu_l\phi_j)]^k_i = (\nu_k\psi_i, \mathbb{G}(\mu_l\phi_j))_{\mathcal{Y}}. \tag{3.3}$$

REMARK 3. *Alternatively,* $\mathbf{H}$ *can be considered as a fourth-order tensor in* $\mathbb{R}^{s\times r\times q\times p}$ *with elements* $\mathbf{H}_{ijkl} = \mathbf{H}^{kl}_{ij}$.

To have a discrete analogon of the $\mathscr{L}(\mathcal{U},\mathcal{Y})$-norm, we introduce for given $\mathcal{U}_{h_1,\tau_1}$ and $\mathcal{Y}_{h_2,\tau_2}$ the weighted matrix norm

$$\|\mathbf{G}(h_1,\tau_1,h_2,\tau_2)\|_{qs\times pr;w} := \sup_{\mathbf{u}\in\mathbb{R}^{pr}} \frac{\|\mathbf{G}\mathbf{u}\|_{qs;w}}{\|\mathbf{u}\|_{pr;w}} = \|\mathbf{M}^{1/2}_{\mathcal{Y},h_2,\tau_2}\mathbf{G}\mathbf{M}^{-1/2}_{\mathcal{U},h_1,\tau_1}\|_{qs\times pr}, \tag{3.4}$$

and we write $(h_1',\tau_1',h_2',\tau_2') \le (h_1,\tau_1,h_2,\tau_2)$ if the inequality holds component-wise.

LEMMA 3.1. *For all* $(h_1,\tau_1,h_2,\tau_2) \in \mathbb{R}^4_+$, *we have*

$$\|\mathbf{G}(h_1,\tau_1,h_2,\tau_2)\|_{qs\times pr;w} = \|\mathbb{G}_S(h_1,\tau_1,h_2,\tau_2)\|_{\mathscr{L}(\mathcal{U},\mathcal{Y})} \le \|\mathbb{G}\|_{\mathscr{L}(\mathcal{U},\mathcal{Y})}. \tag{3.5}$$

If the subspaces $\{\mathcal{U}_{h_1,\tau_1}\}_{h_1,\tau_1>0}$ *and* $\{\mathcal{Y}_{h_2,\tau_2}\}_{h_2,\tau_2>0}$ *are nested in the sense that*

$$\mathcal{U}_{h_1,\tau_1} \subset \mathcal{U}_{h_1',\tau_1'}, \quad \mathcal{Y}_{h_2,\tau_2} \subset \mathcal{Y}_{h_2',\tau_2'} \quad \textit{for } (h_1',\tau_1',h_2',\tau_2') \le (h_1,\tau_1,h_2,\tau_2), \tag{3.6}$$

then $\|\mathbf{G}(h_1,\tau_1,h_2,\tau_2)\|_{qs\times pr;w}$ *monotonically increases for decreasing* $(h_1,\tau_1,h_2,\tau_2) \in \mathbb{R}^4_+$, *and* $\|\mathbf{G}(h_1,\tau_1,h_2,\tau_2)\|_{qs\times pr;w}$ *is convergent for* $(h_1,\tau_1,h_2,\tau_2) \searrow 0$.

Proof. In order to show (3.5), we calculate

$$\|\mathbb{G}_S\|_{\mathscr{L}(\mathcal{U},\mathcal{Y})} = \sup_{u\in\mathcal{U}_{h_1,\tau_1}} \frac{\|\mathbb{P}_{\mathcal{Y},h_2,\tau_2}\mathbb{G}u\|_{\mathcal{Y}}}{\|u\|_{\mathcal{U}}} \le \sup_{u\in\mathcal{U}_{h_1,\tau_1}} \frac{\|\mathbb{G}u\|_{\mathcal{Y}}}{\|u\|_{\mathcal{U}}} \le \|\mathbb{G}\|_{\mathscr{L}(\mathcal{U},\mathcal{Y})},$$

and observe that for $u \in \mathcal{U}_{h_1,\tau_1}$ and $\mathbf{u} = \kappa_{\mathcal{U},h_1,\tau_1}u \in \mathbb{R}^{pr}$, we have

$$\|\mathbb{G}_S u\|_{\mathcal{Y}} = \|\kappa^{-1}_{\mathcal{Y},h_2,\tau_2}\mathbf{G}\kappa_{\mathcal{U},h_1,\tau_1}\mathbb{P}_{\mathcal{U},h_1,\tau_1}u\|_{\mathcal{Y}} = \|\mathbf{G}\mathbf{u}\|_{qs;w} \le \|\mathbf{G}\|_{qs\times pr;w}\|u\|_{\mathcal{U}},$$
$$\|\mathbf{G}\mathbf{u}\|_{qs;w} \le \|\kappa_{\mathcal{Y},h_2,\tau_2}\mathbb{G}_S\kappa^{-1}_{\mathcal{U},h_1,\tau_1}\mathbf{u}\|_{qs;w} = \|\mathbb{G}_S u\|_{\mathcal{Y}} \le \|\mathbb{G}_S\|_{\mathscr{L}(\mathcal{U},\mathcal{Y}}\|\mathbf{u}\|_{pr;w}.$$

Assume that (3.6) holds. Since $\|\mathbb{P}_{\mathcal{Y},h_2,\tau_2}y\|_{\mathcal{Y}} \le \|\mathbb{P}_{\mathcal{Y},h_2',\tau_2'}y\|_{\mathcal{Y}}$ for all $y \in \mathcal{Y}$, we have

$$\|\mathbb{G}_S(h_1,\tau_1,h_2,\tau_2)\|_{qs\times pr;w} \le \sup_{u\in\mathcal{U}_{h_1',\tau_1'}} \frac{\|\mathbb{P}_{\mathcal{Y},h_2',\tau_2'}\mathbb{G}u\|_{\mathcal{Y}}}{\|u\|_{\mathcal{U}}} = \|\mathbb{G}_S(h_1',\tau_1',h_2',\tau_2')\|_{q's'\times p'r';w}.$$

Hence, (3.5) ensures the convergence of $\|\mathbb{G}_S(\mathbf{h})\|_{qs\times pr;w}$. ∎

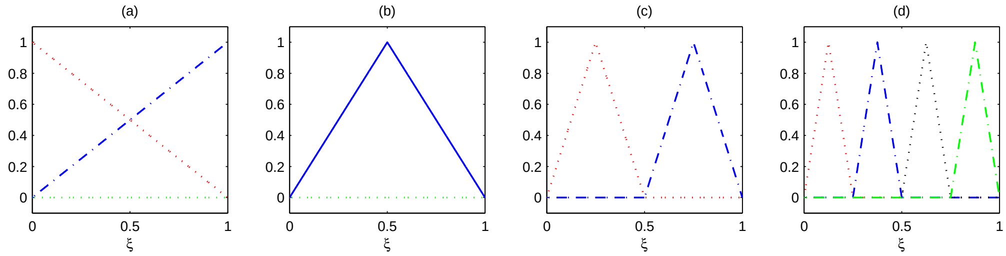

FIG. 3.1. *Hierarchical basis for $L^2(0,1)$-subspaces of piecewise linear functions: (a) μ_1 and μ_2 (b) μ_3 (c) μ_4 and μ_5 (d) $\mu_6, \dots, \mu_9$.*

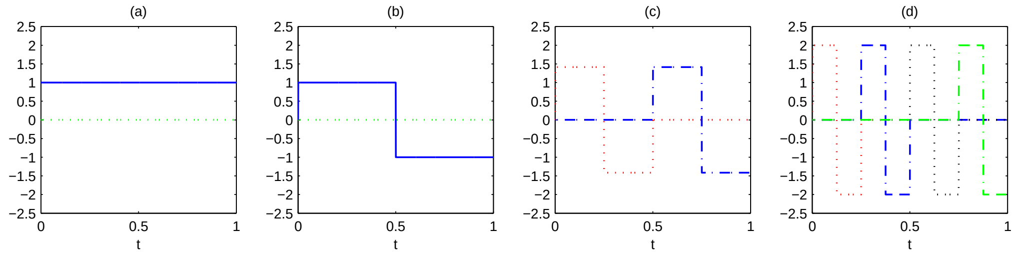

FIG. 3.2. *Haar wavelet basis for $L^2(0,1)$-subspaces of piecewise constant functions: (a) ϕ_1 (b) ϕ_2 (c) ϕ_3 and ϕ_4 (d) $\phi_5, \dots, \phi_8$.*

3.2. An example for signal discretizations. As an example, consider the case $U = Y = L^2(0,1)$, and choose U_{h_1} and Y_{h_2} as spaces of continuous piecewise linear functions and $\mathcal{R}_{\tau_1}$ and $\mathcal{S}_{\tau_2}$ as spaces of piecewise constant functions, all with respect to equidistant grids.

For $p \in \mathbb{N}$, $p \geq 2$ and $h_1(p) = 1/(p-1)$, let $\mathscr{T}_{h_1} = \{I_k\}_{1\leq k\leq p-1}$ be the equidistant partition of $(0,1]$ into intervals $I_k = ((k-1)h_1, kh_1]$. The corresponding space U_{h_1} of continuous piecewise linear functions is, for instance, spanned by the nodal basis

$$\{\mu_1^{(h_1)}, \dots, \mu_{p(h_1)}^{(h_1)}\} \subset U_{h_1}, \quad \text{with } \mu_l^{(h_1)}(kh_1) = \delta_{l-1}(k), \quad k = 0, \dots, p,$$

i.e. the $\mu_k^{(h_1)}$ are the well-known hat functions. The subspaces $\{U_{h_1}\}$ are nested if the choice is restricted to $h_1 \in \{2^{-n}\}_{n\in\mathbb{N}_0}$ and $p \in \{2^n + 1\}_{n\in\mathbb{N}_0}$. Since the *nodal* bases of U_{h_1} and $U_{h_1'}$ do not have any common element for $h_1 \neq h_1'$, one may prefer to choose a *hierarchical* basis of finite element functions $\hat{\mu}_l$, as in Fig. 3.1, see e.g. [49], [50]. Then, $U_{h_1} = \text{span}\{\hat{\mu}_1, \dots, \hat{\mu}_{p(h_1)}\}$ for all $h_1 \in \{2^{-n}\}_{n\in\mathbb{N}_0}$ with basis functions $\hat{\mu}_k$ independent of h_1.

For $r \in \mathbb{N}$ and $\tau_1 = T/r$, let $\Gamma_{\tau_1} = \{I_j\}_{1\leq j\leq r}$ be the equidistant partition of $(0,T]$ into intervals $I_j = ((j-1)\tau_1, j\tau_1]$. The corresponding space $\mathcal{R}_{\tau_1}$ of piecewise constant functions is, for instance, spanned by the nodal and orthogonal basis

$$\{\phi_1^{(\tau_1)}(t), \dots, \phi_r^{(\tau_1)}(t)\}, \quad \text{with } \phi_j^{(\tau_1)}(t) = \chi_{I_j}(t), \qquad j = 1, \dots, r. \tag{3.7}$$

The spaces are nested by requiring $\tau_1 \in \{2^{-n}T\}_{n\in\mathbb{N}_0}$. An orthonormal hierarchical basis for $\mathcal{R}_{\tau_1}$ is obtained by choosing ϕ_j as Haar-wavelets, cf. Fig. 3.2 and [17].

Denoting the orthogonal projections onto U_{h_1} and $\mathcal{R}_{\tau_1}$ by P_{U,h_1} and $P_{\mathcal{R},\tau_1}$, respectively, the Poincaré-Friedrich's inequality shows that there exist constants $c_U = 1/2$

and $c_{\mathcal{R}} = 1/\sqrt{2}$, independent of h_1, τ_1 and T, such that

$$\|u - P_{U_{h_1}} u\|_{L^2(0,1)} \leq c_U h_1^2 \|\partial_\xi^2 u\|_{L^2(0,1)} \quad \text{for } u \in H^2(0,1), \tag{3.8a}$$

$$\|v - P_{\mathcal{R}_{\tau_1}} v\|_{L^2(0,T)} \leq c_{\mathcal{R}} \tau_1 \|\partial_t v\|_{L^2(0,T)} \quad \text{for } v \in H^1(0,T), \tag{3.8b}$$

see e.g. [16, 51]. By Fubini's theorem, it follows that the corresponding projection $\mathbb{P}_{\mathcal{U},h_1,\tau_1}$ onto $\mathcal{U}_{h_1,\tau_1} = \{u \in \mathcal{U},\ u_{|I_j} \equiv u^{(j)},\ u^{(j)} \in U_{h_1},\quad j = 1,\dots,r\}$ satisfies

$$\|u - \mathbb{P}_{\mathcal{U},h_1,\tau_1} u\|_{\mathcal{U}} \leq (c_U h_1^2 + c_{\mathcal{R}} \tau_1)\|u\|_{\mathcal{U}_s} \quad \text{for all } u \in \mathcal{U}_s = H^{1,2}((0,T)\times(0,1)). \tag{3.9}$$

We define $Y_{h_2}, \mathcal{R}_{\tau_2}$ and $\mathcal{Y}_{h_2,\tau_2}$ accordingly and a corresponding estimate as (3.9) holds for the projection $\mathbb{P}_{\mathcal{Y},h_2,\tau_2} y$ of elements $y \in \mathcal{Y}_s = \mathcal{U}_s$.

REMARK 4. *Estimates similar to* (3.9) *also exist for domains* $\Theta \subset \mathbb{R}^d$ *with* $d \geq 1$ *and are classical results from the interpolation theory in Sobolev spaces, see e.g. [16]. Note that the interpolation constants then often have to be estimated numerically. Estimates with higher approximation orders can be obtained, if ansatz functions of higher polynomial degree are used and if the input and output signals exhibit corresponding higher regularity in space and time.*

3.3. Interpretation as discrete-time multi-input-multi-output system. $\mathbb{G}_S$ can be considered as a generalization of a classical linear *discrete-time multi-input-multi-output* (MIMO) system. Input signals $u \in \mathcal{U}_{h_1,\tau_1}$ and output signals $y \in \mathcal{Y}_{h_2,\tau_2}$ can be uniquely represented by finite sequences

$$\{\mathbf{u}_1,\dots,\mathbf{u}_r\} \subset \mathbb{R}^p, \qquad \{\tilde{\mathbf{y}}_1,\dots,\tilde{\mathbf{y}}_s\} \subset \mathbb{R}^q,$$

with coefficient vectors $\mathbf{u}_i = (\mathbf{u}_i^1,\dots,\mathbf{u}_i^p)^T$ and $\tilde{\mathbf{y}}_i = (\tilde{\mathbf{y}}_i^1,\dots,\tilde{\mathbf{y}}_i^q)^T$, where $\mathbf{u} = \kappa_{\mathcal{U},h_1,\tau_1} u$ and $\tilde{\mathbf{y}} = \mathbf{M}_{\mathcal{Y},h_2,\tau_2} \kappa_{\mathcal{Y},h_2,\tau_2} y$. Hence, $y = \mathbb{G}_S u$ writes as

$$\Sigma: \quad \tilde{\mathbf{y}}_i = \sum_{j\in\mathbb{Z}} \mathbf{H}_{ij} \mathbf{u}_j, \quad i \in \mathbb{Z}, \tag{3.10}$$

where $\mathbf{H}_{ij} = [\mathbf{H}_{ij}^{kl}]_{kl} \in \mathbb{R}^{q\times p}$ for $1 \leq i \leq s$ and $1 \leq j \leq r$, and we define $\mathbf{H}_{ij} := 0 \in \mathbb{R}^{q\times p}$ for other $i, j \in \mathbb{Z}$. (3.10) is the external representation of a general linear discrete-time system Σ with p input channels and q output channels, see e.g. [2]. In this context, $\mathbf{u}_j$ (resp. $\tilde{\mathbf{y}}_j$) usually denotes the input value (resp. output value) at the point of time $t_j = j\tau$ with some fixed time step size τ. Σ is called *causal* if $\mathbf{H}_{ij} = 0$ for $j > i$ and Σ is called *time-invariant* if $\mathbf{H}_{ij} = \mathbf{H}_{i-j}$. For a time-invariant system, the sequence of $q\times p$ constant matrices $h_\Sigma = (\dots,\mathbf{H}_{-2},\mathbf{H}_{-1},\mathbf{H}_0,\mathbf{H}_1,\mathbf{H}_2,\dots)$ is called the *impulse response* of Σ because it is the output obtained to a unit impulse $\mathbf{u}_j = \delta_0(j)$. For a causal time-invariant system, the matrices $\mathbf{H}_0, \mathbf{H}_1, \dots$ are often referred to as the *Markov parameters* of Σ.

The causality and time-invariance of the i/o-map $\mathbb{G}$ (cf. Rem. 1) transfer to the causality and time-invariance of Σ if the time basis functions ϕ_j and ψ_i are chosen in an appropriate way. Choosing, for instance, $\phi_1 = \psi_1, \dots, \phi_r = \psi_r$ as in (3.7) for some $r = s \in \mathbb{N}$ and $\tau = \tau_1 = \tau_2 = 1/r$, the matrices $\mathbf{H}^{kl} \in \mathbb{R}^{r\times r}$ are lower triangular Toeplitz matrices and $\mathbf{u}_j$ and $\tilde{\mathbf{y}}_j$ can be interpreted as signal values at time $t_j = j\tau$, cf. Remark 7. Note that all ϕ_j and ψ_i satisfying $\phi_j = \sigma_{(j-1)\tau}\phi_1$ and $\psi_i = \sigma_{(i-1)\tau}\psi_1$ will also ensure this property.

The problem of finding an *internal* or *state space representation* of Σ with minimal state space dimension is referred to as *minimal partial realization* problem, and in particular for causal time-invariant systems, many algorithms exist to solve it, see e.g. [13, 21, 39].

3.4. Signal approximation error estimates. We first consider the signal error ϵ_D with respect to the $\mathscr{L}(\mathcal{U},\mathcal{Y})$-norm.

LEMMA 3.2. *The signal approximation error $\epsilon_s := \|\mathbb{G}-\mathbb{G}_S\|_{\mathscr{L}(\mathcal{U},\mathcal{Y})}$ decomposes into $\epsilon_s = \epsilon_{s,inp}+\epsilon_{s,outp}$ with*

$$\epsilon_{s,inp} := \sup_{u\in \ker \mathbb{P}_{\mathcal{U},h_1,\tau_1}} \frac{\|\mathbb{G}u\|_{\mathcal{Y}}}{\|u\|_{\mathcal{U}}}, \quad \epsilon_{s,outp} := \max_{u\in\mathcal{U}_{h_1,\tau_1}} \frac{\|(I-\mathbb{P}_{\mathcal{Y},h_2,\tau_2})\mathbb{G}u)\|_{\mathcal{Y}}}{\|u\|_{\mathcal{U}}}.$$

Proof. We estimate

$$\epsilon_s \leq \|\mathbb{G}(\mathbb{I}-\mathbb{P}_{\mathcal{U},h_1,\tau_1})\|_{\mathscr{L}(\mathcal{U},\mathcal{Y})} + \|(\mathbb{I}-\mathbb{P}_{\mathcal{Y},h_2,\tau_2})\mathbb{G}\mathbb{P}_{\mathcal{U},h_1,\tau_1}\|_{\mathscr{L}(\mathcal{U},\mathcal{Y})} \tag{3.11}$$

and observe that

$$\epsilon_{s,outp} = \|(\mathbb{I}-\mathbb{P}_{\mathcal{Y},h_2,\tau_2})\mathbb{G}\mathbb{P}_{\mathcal{U},h_1,\tau_1}\|_{\mathscr{L}(\mathcal{U},\mathcal{Y})}, \qquad \epsilon_{s,inp} = \|\mathbb{G}(\mathbb{I}-\mathbb{P}_{\mathcal{U},h_1,\tau_1})\|_{\mathscr{L}(\mathcal{U},\mathcal{Y})}.$$

We obtain the equality in (3.11) by considering a sequence $u_j = u^* + u_j'$, where u^* is the maximizer in the definition of $\epsilon_{s,outp}$ and $(u_j')_j \subset \ker\mathbb{P}_{\mathcal{U},h_1,\tau_1}$ is a supremal sequence in the definition of $\epsilon_{s,inp}$. □

The next remarks show that we can only hope for a good approximation in $\|\cdot\|_{\mathscr{L}(\mathcal{U},\mathcal{Y})}$ if the subspaces $\mathcal{U}_{h_1,\tau_1}$ and $\mathcal{Y}_{h_2,\tau_2}$ can be chosen *specifically* for $\mathbb{G}$ such that output signals from input signals $u\in\mathcal{U}_{h_1,\tau_1}$ are well approximated in $\mathcal{Y}_{h_2,\tau_2}$ and that neglected input signal components in $\ker\mathbb{P}_{\mathcal{U},h_1,\tau_1}$ only lead to small output signals.

REMARK 5. *A usual requirement for families of approximating subspaces $\mathcal{U}_{h_1,\tau_1}$ and $\mathcal{Y}_{h_2,\tau_2}$ is that they become dense if $h_1,\tau_1,h_2,\tau_2\to 0$. We note that this condition implies that $\|(\mathbb{G}-\mathbb{G}_S)u\|_{\mathcal{Y}}\to 0$ for every $u\in\mathcal{U}$, but does* not *guarantee the* uniform convergence *$\|\mathbb{G}-\mathbb{G}_S\|_{\mathscr{L}(\mathcal{U},\mathcal{Y})}\to 0$. Considering, for instance, the identity operator $\mathbb{G}=Id\in\mathscr{L}(\mathcal{U},\mathcal{Y})$ in the case $\mathcal{U}=\mathcal{Y}$, $\epsilon_{s,inp}$ equals one for every finite-dimensional $\mathcal{U}_{h_1,\tau_1}$. Similar effects can be expected for operators with feedthrough components acting between infinite-dimensional subspaces.*

REMARK 6. *If $\mathbb{G}\in\mathscr{L}(\mathcal{U},\mathcal{Y})$ is a compact operator, then there exist orthonormal systems $\{\hat u_1,\hat u_2\dots\}$ of $\mathcal{U}$ and $\{\hat y_1,\hat y_2,\dots\}$ of $\mathcal{Y}$ and nonnegative numbers $\sigma_1\geq\sigma_2\geq\dots$ with $\sigma_k\to 0$ such that $\mathbb{G}u=\sum_{k=1}^\infty \sigma_k(u,\hat u_k)_{\mathcal{U}}\hat y_k$ for all $u\in\mathcal{U}$, see e.g. [47]. Choosing $\mathcal{U}_{h_1,\tau_1}$ and $\mathcal{Y}_{h_2,\tau_2}$ as the span of $\hat u_1,\dots,\hat u_r$ and $\hat y_1,\dots,\hat y_s$, respectively, with $s=r$ and $r\in\mathbb{N}$, we obtain an efficient approximation $\mathbb{G}_S$ of $\mathbb{G}$ with $\|\mathbb{G}-\mathbb{G}_S\|_{\mathscr{L}(\mathcal{U},\mathcal{Y})}\leq\sigma_{r+1}$.*

The case where less specific information about $\mathbb{G}$ is available and we only know that $\mathbb{G}_{|\mathcal{U}_s}\in\mathscr{L}(\mathcal{U}_s,\mathcal{Y}_s)$ with spaces of higher regularity in space and time $\mathcal{U}_s\subset\mathcal{U}$ and $\mathcal{Y}_s\subset\mathcal{Y}$ like in Example 1 will be considered in Theorem 5.1.

4. Approximation of system dynamics. We discuss the efficient approximation of $\mathbb{G}_S$ respectively of its matrix representation $\mathbf{G}=\mathbf{M}_{\mathcal{Y}}^{-1}\mathbf{H}$. For time-invariant systems with distributed control and observation, this task reduces to the approximation of the convolution kernel $K\in L^2(0,T;\mathscr{L}(U,Y))$.

4.1. Kernel function approximation. Inserting (2.4) in (3.3), by a change of variables we obtain

$$\mathbf{H}_{ij}^{kl} = \int_0^T\int_0^T \psi_i(t)\phi_j(s)(\nu_k, K(t-s)\mu_l)_Y\,ds\,dt = \int_0^T \mathbf{W}_{ij}(t)\mathbf{K}_{kl}(t)\,dt$$

with matrix-valued functions $\mathbf{W} : [0,T] \to \mathbb{R}^{s\times r}$ and $\mathbf{K} : [0,T] \to \mathbb{R}^{q\times p}$,

$$\mathbf{W}_{ij}(t) = \int_0^{T-t} \psi_i(t+s)\phi_j(s)\,ds, \qquad \mathbf{K}_{kl}(t) = (\nu_k, K(t)\mu_l)_Y,$$

and thus

$$\mathbf{H} = \mathbf{M}_{\mathcal{Y}}\mathbf{G} = \int_0^T \mathbf{K}(t) \otimes \mathbf{W}(t)\,dt. \tag{4.2}$$

REMARK 7. $\mathbf{W}(t)$ *can be exactly calculated if piecewise polynomial ansatz functions* $\psi_i(t)$ *and* $\phi_j(t)$ *are chosen. For the special choice* (3.7)*, we see in this way that* $\mathbf{W}(t) \in \mathbb{R}^{r\times r}$ *is a lower triangular Toeplitz matrix for all* $t \in [0,T]$*, and hence the matrices* $\mathbf{H}_{ij} = \int_0^T \mathbf{W}_{ij}(t)\mathbf{K}(t)\,dt \in \mathbb{R}^{q\times p}$ *satisfy* $\mathbf{H}_{ij} = \mathbf{H}_{i-j}$ *for* $1 \le i,j \le r$ *and* $\mathbf{H}_{ij} = 0$ *for* $1 \le i < j \le r$*. In view of Section 3.3, the* $\mathbf{H}_{ij}$ *are thus the* Markov parameters *of a* discrete-time linear time-invariant causal *MIMO system.*

For systems of the form (2.1), the matrix-valued function $\mathbf{K}$ is given by

$$\mathbf{K}_{kl}(t) = (\nu_k, CS(t)B\mu_l)_Y = (c_k^*, S(t)b_l)_Z,$$

where $c_k^* = C^*\nu_k \in Z$ and $b_l = B\mu_l$ for $k = 1,\dots,q$ and $l = 1,\dots,p$. Hence, $\mathbf{K}$ can be calculated by solving p homogeneous systems

$$\dot{z}_l(t) = Az_l(t), \qquad t \in (0,T], \tag{4.3a}$$

$$z_l(0) = b_l, \tag{4.3b}$$

since (4.3) has the mild solution $z_l(t) = S(t)b_l \in C([0,T];L^2(\Omega))$. We obtain an approximation $\tilde{\mathbf{H}}$ of $\mathbf{H}$ by replacing $z_l(t)$ by numerical approximations $z_{l,\mathtt{tol}}(t)$, i.e.

$$\tilde{\mathbf{H}} = \int_0^T \tilde{\mathbf{K}}(t) \otimes \mathbf{W}(t)\,dt, \tag{4.4}$$

with $\tilde{\mathbf{K}}_{kl}(t) = (\nu_k, Cz_{l,\mathtt{tol}}(t))_Y = (c_k^*, z_{l,\mathtt{tol}}(t))_Z$. Here the subscript `tol` indicates that the error $z_l - z_{l,\mathtt{tol}}$ is assumed to satisfy some tolerance criterion which will be specified later. The corresponding approximation $\mathbb{G}_{DS}$ of $\mathbb{G}_S$ is given by

$$\mathbb{G}_{DS} = \kappa_{\mathcal{Y}}^{-1}\tilde{\mathbf{G}}\kappa_{\mathcal{U}}\mathbb{P}_{\mathcal{U}}, \quad \text{with } \tilde{\mathbf{G}} = \mathbf{M}_{\mathcal{Y}}^{-1}\tilde{\mathbf{H}} \tag{4.5}$$

and depends on h_1, h_2, τ_1, τ_2 and `tol`.

REMARK 8. *The matrix function* $\mathbf{K}$ *is approximated* column-wise. *The kernel may also be calculated* row-wise *by solving an adjoint autonomous system, which may be preferable if* $q < p$ *or if the output approximation is successively improved by adding further basis functions* $\nu_{q+1}, \nu_{q+2}, \dots$*.*

REMARK 9. *The calculation of* $\tilde{\mathbf{H}}$ *can be parallelized in an obvious way by calculating the* p *solutions* $z_{l,\mathtt{tol}}$ *in parallel and we note that no state trajectories have to be stored. In general, the matrix* $\tilde{\mathbf{H}}$ *is not sparse, such that the memory requirements become significant if a high resolution of the signals in space and time is required, and the question of a data-sparse representation arises. Recalling Remark 7, the blocks* $\tilde{\mathbf{H}}^{kl}$ *are lower triangular Toeplitz matrices for the special choice of time basis funtions* (3.7) *and thus only* $q\cdot p\cdot r$ *elements have to be stored. Another approach to obtain data-sparse representations uses approximate factorizations* $\check{\mathbf{K}}_{kl}(t-s) = \sum_{m,n=1}^M \alpha_{mn}L_m(t)L_n(s)$ *for* $s,t \in [0,T]$ *with suitable ansatz functions* $L_n(t)$*, see e.g. [29].*

4.2. Dynamics approximation error. The following proposition relates the system dynamics error ϵ_D to the errors made in solving the PDE (4.3) for $l = 1, \dots, p$.

PROPOSITION 4.1. *The system dynamics error* $\epsilon_D := \|\mathbb{G}_S - \mathbb{G}_{DS}\|_{\mathscr{L}(\mathcal{U},\mathcal{Y})}$ *satisfies*

$$\epsilon_D \leq \sqrt{T}\|\mathbf{K} - \tilde{\mathbf{K}}\|_{L^2(0,T;\mathbb{R}^{q\times p}_w)} \leq p\sqrt{T}\sqrt{\frac{\lambda_{\max}(\mathbf{M}_{Y,h_2})}{\lambda_{\min}(\mathbf{M}_{U,h_1})}} \max_{1\leq l\leq p} \|\mathbf{K}_{:,l} - \tilde{\mathbf{K}}_{:,l}\|_{L^2(0,T;\mathbb{R}^q)}. \tag{4.6}$$

Here $\mathbf{K}_{:,l}$ *and* $\tilde{\mathbf{K}}_{:,l}$ *denote the l'th column of* $\mathbf{K}(t)$ *and* $\tilde{\mathbf{K}}(t)$*, respectively,* $\lambda_{\max}(\mathbf{M}_{Y,h_2})$ *is the largest eigenvalue of* $\mathbf{M}_{Y,h_2}$ *and* $\lambda_{\min}(\mathbf{M}_{U,h_1})$ *the smallest eigenvalue of* $\mathbf{M}_{U,h_1}$*.* $\mathbb{R}^{q\times p}_w$ *denotes the space of real* $q \times p$*-matrices equipped with the weighted matrix norm* $\|\mathbf{M}\|_{q\times p;w} = \sup_{\mathbf{u}\neq 0} \|\mathbf{M}\mathbf{u}\|_{q;w}/\|\mathbf{u}\|_{p;w}$*.*

Proof. $\mathbf{K}$ is the matrix function representation of the space-projected kernel function $K_m : [-T,T] \to \mathscr{L}(U,Y)$ with $K_m(t) = P_{Y,h_2}K(t)P_{U,h_1}$, where P_{Y,h_2} and P_{U,h_1} are the orthogonal projections onto the subspaces Y_{h_2} and U_{h_1}, respectively. Introducing the corresponding i/o-map $\mathbb{G}_m = \mathbb{G}_m(h_1,h_2)$,

$$(\mathbb{G}_m u)(t) = \int_0^T K_m(t-s)u(s)\,ds, \qquad t \in [0,T]. \tag{4.7}$$

we note that $\mathbb{G}_S = \mathbb{P}_{\mathcal{Y},h_2,\tau_2}\mathbb{G}_m\mathbb{P}_{\mathcal{U},h_1,\tau_1}$. Similarly, we associate with $\tilde{\mathbf{K}}(t)$ the kernel function $\tilde{K} : [-T,T] \to \mathscr{L}(U,Y)$ with $\tilde{K}(t) = \kappa^{-1}_{Y,h_2}\tilde{\mathbf{K}}(t)\kappa_{U,h_1}P_{U,h_1}$, and with corresponding i/o-map

$$(\mathbb{G}_D u)(t) = \int_0^T \tilde{K}(t-s)u(s)\,ds, \qquad t \in [0,T]. \tag{4.8}$$

We observe that $\mathbb{G}_{DS}$ as defined in (4.5) satisfies $\mathbb{G}_{DS} = \mathbb{P}_{\mathcal{Y},h_2,\tau_2}\mathbb{G}_D\mathbb{P}_{\mathcal{U},h_1,\tau_1}$ by showing according to (3.2)-(4.2) that the matrix representation of $\mathbb{P}_{\mathcal{Y},h_2,\tau_2}\mathbb{G}_D\mathbb{P}_{\mathcal{U},h_1,\tau_1}$ coincides with (4.4). We note that $\|K_m(t)\|_{\mathscr{L}(U,Y)} = \|\mathbf{K}(t)\|_{q\times p;w}$ and $\|\tilde{K}(t)\|_{\mathscr{L}(U,Y)} = \|\tilde{\mathbf{K}}(t)\|_{q\times p;w}$ for all $t \in [0,T]$. Lemma 2.1 yields

$$\|\mathbb{G}_m - \mathbb{G}_D\|_{\mathscr{L}(\mathcal{U},\mathcal{Y})} \leq \sqrt{T}\|K_m - \tilde{K}\|_{L^2(0,T;\mathscr{L}(U,Y))} = \sqrt{T}\|\mathbf{K} - \tilde{\mathbf{K}}\|_{L^2(0,T;\mathbb{R}^{q\times p}_w)}.$$

Defining $\mathbf{E}(t) = \mathbf{K}(t) - \tilde{\mathbf{K}}(t)$, for $\mathbf{u} \in \mathbb{R}^p$ with $\|\mathbf{u}\|_{\mathbb{R}^p} = 1$ and $t \in [0,T]$, by using the equivalence of the 1−norm and 2-vector norms in $\mathbb{R}^p$ we have that

$$\|\mathbf{E}(t)\mathbf{u}\|_{\mathbb{R}^q} \leq \sum_{l=1}^p |\mathbf{u}_l|\|\mathbf{E}_{:,l}(t)\|_{\mathbb{R}^q} \leq \sqrt{p}\left(\sum_{l=1}^p \|\mathbf{E}_{:,l}(t)\|^2_{\mathbb{R}^q}\right)^{1/2}$$

and hence $\|\mathbf{E}\|^2_{L^2(0,T;\mathbb{R}^{q\times p})} \leq p\sum_{l=1}^p \int_0^T \|\mathbf{E}_{:,l}(t)\|^2_{\mathbb{R}^q}\,dt \leq p^2 \max_{l=1,\dots,p} \int_0^T \|\mathbf{E}_{:,l}(t)\|^2_{\mathbb{R}^q}\,dt$, which concludes the proof. □

REMARK 10. *Calculating directly the columns of* $\mathbf{K}$ *and estimating* ϵ_D *via* (4.6)*, the quotient of the eigenvalues of the mass matrices* $\mathbf{M}_{U,h_1}$ *and* $\mathbf{M}_{Y,h_2}$ *has to be compensated by the approximation accuracy of* $\mathbf{K}_{:,l}$*. This may be problematic if hierarchical basis functions are chosen, since the quotient grows unboundedly with decreasing* h_1 *and* h_2*. One may circumvent this problem by calculating* $\mathbf{K}$ *with respect to different bases. Approximating the columns of* $\mathbf{K}^w(t) = \mathbf{M}^{1/2}_{\mathcal{Y}}\mathbf{K}(t)\mathbf{M}^{-1/2}_{\mathcal{U}}$ *via an adapted problem* (4.3)*, we have* $\epsilon_D \leq p\sqrt{T}\max_{1\leq l\leq p}\|\mathbf{K}^w_{:,l} - \tilde{\mathbf{K}}^w_{:,l}\|_{L^2(0,T;\mathbb{R}^q)}$*. Note that the necessary back transformations have to be carried out with sufficient accuracy.*

4.3. Error estimation for the homogeneous PDE. In order to approximate the system dynamics, the homogeneous PDE (4.3) has to be solved via a fully-discrete numerical scheme for p different initial values. A *first* goal is to choose the time and space grids (and possibly other discretization parameters) such that

$$\|\mathbf{K}_{:,l} - \tilde{\mathbf{K}}_{:,l}\|_{L^2(0,T;\mathbb{R}^q)} < \texttt{tol} \quad \text{resp.} \quad \|\mathbf{K}^w_{:,l} - \tilde{\mathbf{K}}^w_{:,l}\|_{L^2(0,T;\mathbb{R}^q)} < \texttt{tol} \tag{4.9}$$

is *guaranteed* for a given $\texttt{tol} > 0$ by means of reliable error estimators. A *second* goal is to achieve this accuracy in a *cost-economic* way. A special difficulty in solving (4.3) numerically is the handling of initial values b_l, which belong in general only to Z but not necessarily to $D(A)$. Considering the example heat equation, this means that the space and time derivatives of the exact solution $z_l \in C^1((0,T], H^2(\Omega) \cap H^1_0(\Omega))$ may become very large for small t, but decay quickly for $t > 0$. In fact, in general we only have the analytical bound

$$\|\partial_t z(t)\|_{L^2(\Omega)} = \|\triangle z(t)\|_{L^2(\Omega)} \leq \frac{c}{t}\|z^0\|_{L^2(\Omega)} \quad \text{for all } t \in (0,T],$$

with some constant $c > 0$ independent of z_0 and T, cf. [32, p. 148]. Adaptive space and time discretizations on the basis of a posteriori error estimates are the method of choice to match these requirements [23].

Discontinuous Galerkin time discretizations in combination with standard Galerkin space discretizations provide an appropriate framework to derive corresponding (a priori and a posteriori) error estimates, also for the case of adaptively refined grids which are in general no longer quasi-uniform [24, 32, 45]. We distinguish two types of error estimates.

Global state error estimates measure the error $(z_l - z_{l,\texttt{tol}})$ in some global norm. For parabolic problems, a priori and a posteriori estimates for the error in $L^\infty(0,T;L^2(\Omega))$ and $L^\infty(0,T;L^\infty(\Omega))$ can be found in [24]. Such results permit to guarantee (4.9) in view of

$$\|\mathbf{K}_{:,l} - \tilde{\mathbf{K}}_{:,l}\|_{L^2(0,T;\mathbb{R}^q)} \leq \|C\|_{\mathscr{L}(Z,Y)} \left(\sum_{i=1}^{q} \|\nu_i\|_Y^2\right)^{1/2} \|z - z^{(l)}_{\texttt{tol}}\|_{L^2(0,T;Z)}. \tag{4.10}$$

Goal-oriented error estimates can be used to measure the error $\|\mathbf{K}_{:,l} - \tilde{\mathbf{K}}_{:,l}\|_{L^2(0,T;\mathbb{R}^q)}$ directly. This may be advantageous, since (4.10) may be very conservative: the error in the *observations* $\mathbf{K}_{:,l}$ can be small even if some norm of the *state* error is large. The core of these error estimation techniques is an exact error representation formula, which can be evaluated if one knows the residual and the solution of an auxiliary dual PDE. This so-called *dual-weighted residuals* (DWR) approach goes back to [4], substantial contributions have since then been made in [1], [6], [8], [9], [10], [31], [33], [34] and the references therein. Note that the numerical examples presented later are calculated using adaptive time and space grid refinements on the basis of DWR error estimation techniques.

The previous discussion justifies the following assumption.

Assumption 1. *Given a tolerance* $\texttt{tol} > 0$, *we can ensure (by using appropriate error estimators and mesh refinements) that the solutions* z_l *of* (4.3) *and the solutions* $z_{l,\texttt{tol}}$ *calculated by means of an appropriate fully-discrete numerical scheme satisfy*

$$\|\mathbf{K}_{:,l} - \tilde{\mathbf{K}}_{:,l}\|_{L^2(0,T;\mathbb{R}^q)} < \texttt{tol}, \qquad l = 1, \dots, p. \tag{4.11}$$

5. Total error estimates. We present estimates for the total error in the approximation of $\mathbb{G}$ and of its adjoint $\mathbb{G}^*$. Using general-purpose ansatz spaces $\mathcal{U}_{h_1,\tau_1}$ and $\mathcal{Y}_{h_2,\tau_2}$ for the signal approximation, we only obtain error results in a weaker $\mathscr{L}(\mathcal{U}_s,\mathcal{Y})$-norm respectively $\mathscr{L}(\mathcal{Y}_s,\mathcal{U})$-norm.

THEOREM 5.1. *Consider the i/o map $\mathbb{G} \in \mathscr{L}(\mathcal{U},\mathcal{Y})$ of the infinite-dimensional linear time-invariant system* (2.4) *and assume that*

(i) $\mathbb{G}_{|\mathcal{U}_s} \in \mathscr{L}(\mathcal{U}_s,\mathcal{Y}_s)$ *with spaces of higher regularity in space and time*

$$\mathcal{U}_s = H^{\alpha_1,\beta_1}((0,T)\times\Theta), \quad \mathcal{Y}_s = H^{\alpha_2,\beta_2}((0,T)\times\Xi), \quad \alpha_1,\beta_1,\alpha_2,\beta_2 \in \mathbb{N}.$$

(ii) The families of subspaces $\{\mathcal{U}_{h_1,\tau_1}\}_{h_1,\tau_1}$ *and* $\{\mathcal{Y}_{h_2,\tau_2}\}_{h_2,\tau_2}$ *satisfy*

$$\begin{aligned} \|u - \mathbb{P}_{\mathcal{U},h_1,\tau_1}u\|_{\mathcal{U}} &\le (c_{\mathcal{R}}\tau_1^{\alpha_1} + c_U h_1^{\beta_1})\|u\|_{\mathcal{U}_s}, \qquad u \in \mathcal{U}_s,\\ \|y - \mathbb{P}_{\mathcal{Y},h_2,\tau_2}y\|_{\mathcal{Y}} &\le (c_{\mathcal{S}}\tau_2^{\alpha_2} + c_Y h_2^{\beta_2})\|y\|_{\mathcal{Y}_s}, \qquad y \in \mathcal{Y}_s, \end{aligned}$$

with positive constants $c_{\mathcal{R}}$, $c_{\mathcal{S}}$, c_U and c_Y.

(iii) The error in solving for the state dynamics can be made arbitrarily small, i.e. Assumption 1 holds.

Let $\delta > 0$ be given. Then one can choose subspaces $\mathcal{U}_{h_1^*,\tau_1^*}$ and $\mathcal{Y}_{h_2^*,\tau_2^*}$ such that

$$\tau_1^* < \left(\frac{\delta}{8c_{\mathcal{R}}\|\mathbb{G}\|_{\mathscr{L}(\mathcal{U},\mathcal{Y})}}\right)^{1/\alpha_1}, \quad h_1^* < \left(\frac{\delta}{8c_U\|\mathbb{G}\|_{\mathscr{L}(\mathcal{U},\mathcal{Y})}}\right)^{1/\beta_1}, \tag{5.1a}$$

$$\tau_2^* < \left(\frac{\delta}{8c_{\mathcal{S}}\|\mathbb{G}\|_{\mathscr{L}(\mathcal{U}_s,\mathcal{Y}_s)}}\right)^{1/\alpha_2}, \quad h_2^* < \left(\frac{\delta}{8c_Y\|\mathbb{G}\|_{\mathscr{L}(\mathcal{U}_s,\mathcal{Y}_s)}}\right)^{1/\beta_2}, \tag{5.1b}$$

and one can solve numerically the PDEs (4.3) *for $l = 1,\dots,p(h_1)$ such that one of the following conditions holds.*

$$\text{(i)} \qquad \|\mathbf{K}^w_{:,l} - \tilde{\mathbf{K}}^w_{:,l}\|_{L^2(0,T;\mathbb{R}^q)} < \frac{\delta}{2\sqrt{T}p(h_1^*)}, \tag{5.2a}$$

$$\text{(ii)} \qquad \|\mathbf{K}_{:,l} - \tilde{\mathbf{K}}_{:,l}\|_{L^2(0,T;\mathbb{R}^q)} < \frac{\delta}{2\sqrt{T}p(h_1^*)}\sqrt{\frac{\lambda_{\min}(\mathbf{M}_{U,h_1^*})}{\lambda_{\max}(\mathbf{M}_{Y,h_2^*})}}, \tag{5.2b}$$

$$\text{(iii)} \qquad \|z_l - z_{l,\mathtt{tol}}\|_{L^2(0,T;Z)} < \frac{\delta}{2\sqrt{T}p(h_1^*)}\sqrt{\frac{\lambda_{\min}(\mathbf{M}_{U,h_1^*})}{\lambda_{\max}(\mathbf{M}_{Y,h_2^*})}}\|C\|^{-1}_{\mathscr{L}(Z,Y)}\left(\sum_{i=1}^{q(h_2^*)}\|\nu_i\|_Y^2\right)^{-1/2}. \tag{5.2c}$$

In this case,

$$\|\mathbb{G} - \mathbb{G}_{DS}\|_{\mathscr{L}(\mathcal{U}_s,\mathcal{Y})} < \delta.$$

Moreover, the signal error $\epsilon_S' := \|\mathbb{G} - \mathbb{G}_S\|_{\mathscr{L}(\mathcal{U}_s,\mathcal{Y})}$ and the system dynamics error $\epsilon_D := \|\mathbb{G}_S - \mathbb{G}_{DS}\|_{\mathscr{L}(\mathcal{U},\mathcal{Y})}$ are balanced in the sense that $\epsilon_S', \epsilon_D < \delta/2$.

Proof. For $u \in \mathcal{U}_s$, we have

$$\begin{aligned} \|\mathbb{G}u - \mathbb{G}_S u\|_{\mathcal{Y}} &\le \|\mathbb{G}u - \mathbb{P}_{\mathcal{Y},h_2,\tau_2}\mathbb{G}u\|_{\mathcal{Y}} + \|\mathbb{P}_{\mathcal{Y},h_2,\tau_2}\mathbb{G}u - \mathbb{P}_{\mathcal{Y},h_2,\tau_2}\mathbb{G}\mathbb{P}_{\mathcal{U},h_1,\tau_1}u\|_{\mathcal{Y}},\\ &\le (c_{\mathcal{S}}\tau_2^{\alpha_2} + c_Y h_2^{\beta_2})\|\mathbb{G}u\|_{\mathcal{Y}_s} + (c_{\mathcal{R}}\tau_1^{\alpha_1} + c_U h_1^{\beta_1})\|\mathbb{P}_{\mathcal{Y}}\|_{\mathscr{L}(\mathcal{Y})}\|\mathbb{G}\|_{\mathscr{L}(\mathcal{U},\mathcal{Y})}\|u\|_{\mathcal{U}_s},\\ &\le \left\{(c_{\mathcal{S}}\tau_2^{\alpha_2} + c_Y h_2^{\beta_2})\|\mathbb{G}\|_{\mathscr{L}(\mathcal{U}_{rs},\mathcal{Y}_s)} + (c_{\mathcal{R}}\tau_1^{\alpha_1} + c_U h_1^{\beta_1})\|\mathbb{G}\|_{\mathscr{L}(\mathcal{U},\mathcal{Y})}\right\}\|u\|_{\mathcal{U}_s}, \end{aligned}$$

and thus (5.1) ensures that $\epsilon_S' = \|\mathbb{G} - \mathbb{G}_S\|_{\mathscr{L}(\mathcal{U}_s,\mathcal{Y})} < \delta/2$. Proposition 4.1 in combination with (5.2) and in view of (4.10) ensures that $\epsilon_D = \|\mathbb{G}_S - \mathbb{G}_{DS}\|_{\mathscr{L}(\mathcal{U},\mathcal{Y})} < \delta/2$, which concludes the proof. □

REMARK 11. *Condition (i) holds for many systems of practical relevance, cf. Remark 2. Condition (ii) can be achieved by choosing U_{h_1}, Y_{h_2}, $\mathcal{R}_{\tau_1}$ and $\mathcal{S}_{\tau_2}$ for instance as spaces of piecewise polynomial functions of appropriate degrees, cf.* (3.8) *and refer e.g. to [16] for interpolation theory in Sobolev spaces in the case of more general settings.*

REMARK 12. *Considering $\mathbb{G}$ in the $\mathscr{L}(\mathcal{U}_s,\mathcal{Y})$-norm we restrict the input space to input signals of higher regularity in space and time. This is not a strong limitation if we think of $\mathcal{U}_s$ as the space wherein we search for an approximate optimal control, since exact optimal controls exhibit such higher regularity in many applications [46]. Note that we do not exclude the* use *of L^2-controls, in fact, we can consider the spaces $\mathcal{U}_{h_1,\tau_1}$ as spaces of controls which we are able to realize in technical applications.*

In view of (2.9) and (3.9) we can apply Theorem 5.1 to Example 1.

COROLLARY 5.2. *Consider the heat control system in Example 1 with $U = Y = L^2(0,1)$ and let $\delta > 0$ be given. We assume that $C_{|H^2(\Omega)} \in \mathscr{L}(H^2(\Omega), H^2(0,1))$, i.e. $\mathbb{G}_{|\mathcal{U}_s} \in \mathscr{L}(\mathcal{U}_s,\mathcal{Y}_s)$ with $\mathcal{U}_s = \mathcal{Y}_s = H^{1,2}((0,T)\times(0,1)))$. We choose U_{h_1} and Y_{h_2} as spaces of continuous piecewise linear functions with respect to equidistant grids on $[0,1]$, and we choose $\mathcal{R}_{\tau_1}$ and $\mathcal{S}_{\tau_2}$ as spaces of piecewise constant functions with respect to equidistant grids on $[0,T]$, with dimensions satisfying*

$$p > 2\sqrt{\frac{\|\mathbb{G}\|_{\mathscr{L}(\mathcal{U},\mathcal{Y})}}{\delta}} + 1, \quad q > 2\sqrt{\frac{\|\mathbb{G}\|_{\mathscr{L}(\mathcal{U}_s,\mathcal{Y}_s)}}{\delta}} + 1, \tag{5.3a}$$

$$r > \frac{\sqrt{2}4\|\mathbb{G}\|_{\mathscr{L}(\mathcal{U},\mathcal{Y})}}{\delta}, \qquad s > \frac{\sqrt{2}4\|\mathbb{G}\|_{\mathscr{L}(\mathcal{U}_s,\mathcal{Y}_s)}}{\delta}. \tag{5.3b}$$

If the homogeneous heat equations (4.3) *are solved for $l = 1,\dots,p$ such that one of the conditions (i)-(iii) in* (5.2) *holds, then the i/o-maps $\mathbb{G}$ and $\mathbb{G}_{DS}$ restricted to $\mathcal{U}_s$ satisfy*

$$\|\mathbb{G} - \mathbb{G}_{DS}\|_{\mathscr{L}(\mathcal{U}_s,\mathcal{Y})} < \delta.$$

The next result shows that $(\mathbb{G}_{DS})^* \in \mathscr{L}(\mathcal{Y},\mathcal{U})$ automatically approximates the adjoint $\mathbb{G}^*$ with $\|\mathbb{G}^* - (\mathbb{G}_{DS})^*\|_{\mathscr{L}(\mathcal{Y}_s,\mathcal{U})} < c\,\delta$ with a $\mathbb{G}$-specific constant c, under the assumption that $\mathbb{G}^*_{|\mathcal{Y}_s} \in \mathscr{L}(\mathcal{Y}_s,\mathcal{U}_s)$. Note that $\mathbb{G}^* \in \mathscr{L}(\mathcal{Y},\mathcal{U})$ is given by

$$(\mathbb{G}^* y)(s) = \int_0^T K(s-t)^* y(t)dt.$$

THEOREM 5.3. *The adjoint $(\mathbb{G}_{DS})^* \in \mathscr{L}(\mathcal{Y},\mathcal{U})$ of $\mathbb{G}_{DS} \in \mathscr{L}(\mathcal{U},\mathcal{Y})$ has the matrix representation*

$$\tilde{\mathbf{G}}^* := \mathbf{M}_{\mathcal{U}}^{-1}\tilde{\mathbf{G}}^T\mathbf{M}_{\mathcal{Y}} = \mathbf{M}_{\mathcal{U}}^{-1}\tilde{\mathbf{H}}^T \in \mathbb{R}^{pr\times qs} \tag{5.4}$$

For a given $\delta > 0$, assume that all conditions in Theorem 5.1 hold, ensuring that $\|\mathbb{G} - \mathbb{G}_{DS}\|_{\mathscr{L}(\mathcal{U}_s,\mathcal{Y})} < \delta$. If, in addition, $\mathbb{G}^*_{|\mathcal{Y}_s} \in \mathscr{L}(\mathcal{Y}_s,\mathcal{U}_s)$, then

$$\|\mathbb{G}^* - (\mathbb{G}_{DS})^*\|_{\mathscr{L}(\mathcal{Y}_s,\mathcal{U})} < \delta(\frac{1}{2} + c_*) \tag{5.5}$$

with $c_* = \frac{1}{4}(\|\mathbb{G}^*\|_{\mathscr{L}(\mathcal{Y}_s,\mathcal{U}_s)}/\|\mathbb{G}\|_{\mathscr{L}(\mathcal{Y},\mathcal{U})} + \|\mathbb{G}^*\|_{\mathscr{L}(\mathcal{Y},\mathcal{U})}/\|\mathbb{G}\|_{\mathscr{L}(\mathcal{Y}_s,\mathcal{U}_s)})$.

Proof. We first observe that $\tilde{\mathbf{G}}^*$ is the adjoint of $\tilde{\mathbf{G}} : \mathbb{R}^{pr}_w \to \mathbb{R}^{qs}_w$, since

$$(\tilde{\mathbf{G}}\mathbf{u}, \mathbf{y})_{qs;w} = \mathbf{u}^T \tilde{\mathbf{G}}^T \mathbf{M}_{\mathcal{Y}} \mathbf{y} = (\mathbf{u}, \mathbf{M}_{\mathcal{U}}^{-1} \tilde{\mathbf{G}}^T \mathbf{M}_{\mathcal{Y}} \mathbf{y})_{pr;w}.$$

For $u \in \mathcal{U}$ and $y \in \mathcal{Y}$ and omitting the dependencies on h_1, h_2, τ_1, τ_2 and `tol`, we have

$$\begin{aligned}
(\mathbb{G}_{DS}u, y)_{\mathcal{Y}} &= (\mathbb{P}_{\mathcal{Y}}\kappa_{\mathcal{Y}}^{-1}\tilde{\mathbf{G}}\kappa_{\mathcal{U}}\mathbb{P}_{\mathcal{U}}u, y)_{\mathcal{Y}} = (\tilde{\mathbf{G}}\kappa_{\mathcal{U}}\mathbb{P}_{\mathcal{U}}u, \kappa_{\mathcal{Y}}\mathbb{P}_{\mathcal{Y}}y)_{qs;w},\\
&= (\kappa_{\mathcal{U}}\mathbb{P}_{\mathcal{U}}u, \tilde{\mathbf{G}}^*\kappa_{\mathcal{Y}}\mathbb{P}_{\mathcal{Y}}y)_{qs;w} = (u, \mathbb{P}_{\mathcal{U}}\kappa_{\mathcal{U}}^{-1}\tilde{\mathbf{G}}^*\kappa_{\mathcal{Y}}\mathbb{P}_{\mathcal{Y}}y)_{\mathcal{U}},\\
&= (u, (\mathbb{G}_{DS})^*y)_{\mathcal{U}},
\end{aligned}$$

where we have used that $\mathbb{P}_{\mathcal{U}} = \mathbb{P}_{\mathcal{U}}^*$, $\mathbb{P}_{\mathcal{Y}} = \mathbb{P}_{\mathcal{Y}}^*$, $\kappa_{\mathcal{U}}^* = \kappa_{\mathcal{U}}^{-1}$ and $\kappa_{\mathcal{Y}}^* = \kappa_{\mathcal{Y}}^{-1}$. To show (5.5), we estimate

$$\|\mathbb{G}^* - (\mathbb{G}_{DS})^*\|_{\mathscr{L}(\mathcal{Y}_s,\mathcal{U})} \le \|\mathbb{G}^* - (\mathbb{G}_S)^*\|_{\mathscr{L}(\mathcal{Y}_s,\mathcal{U})} + \|\mathbb{G}_S^* - (\mathbb{G}_{DS})^*\|_{\mathscr{L}(\mathcal{Y},\mathcal{U})},$$

where $(\mathbb{G}_S)^* = \mathbb{P}_{\mathcal{U}}\mathbb{G}^*\mathbb{P}_{\mathcal{Y}}$ is the adjoint of $\mathbb{G}_S \in \mathscr{L}(\mathcal{U}, \mathcal{Y})$. In analogy to Thm. 5.1, one shows that

$$\epsilon_S^* := \|\mathbb{G}^* - (\mathbb{G}_S)^*\|_{\mathscr{L}(\mathcal{Y}_s,\mathcal{U})} \le c''_{\mathcal{R}}\tau_1^{\alpha_1} + c''_U h_1^{\beta_1} + c''_{\mathcal{S}}\tau_2^{\alpha_2} + c''_Y h_2^{\beta_2},$$

with $c''_U = \|\mathbb{G}^*\|_{\mathscr{L}(\mathcal{Y}_S,\mathcal{U}_S)}c_U$, $c''_Y = \|\mathbb{G}^*\|_{\mathscr{L}(\mathcal{Y},\mathcal{U})}c_Y$, $c''_{\mathcal{R}} = \|\mathbb{G}^*\|_{\mathscr{L}(\mathcal{Y}_s,\mathcal{U}_s)}c_{\mathcal{R}}$ and $c''_{\mathcal{S}} = \|\mathbb{G}^*\|_{\mathscr{L}(\mathcal{Y},\mathcal{U})}c_{\mathcal{S}}$. Hence, (5.1) implies

$$\epsilon_S^* \le \frac{\delta}{8}\left(\frac{c''_{\mathcal{U}}}{c_{\mathcal{U}}} + \frac{c''_{\mathcal{R}}}{c_{\mathcal{R}}} + \frac{c''_{\mathcal{Y}}}{c_{\mathcal{Y}}} + \frac{c''_{\mathcal{S}}}{c_{\mathcal{S}}}\right) = \frac{\delta}{4}\left(\frac{\|\mathbb{G}^*\|_{\mathscr{L}(\mathcal{Y}_s,\mathcal{U}_s)}}{\|\mathbb{G}\|_{\mathscr{L}(\mathcal{Y},\mathcal{U})}} + \frac{\|\mathbb{G}^*\|_{\mathscr{L}(\mathcal{Y},\mathcal{U})}}{\|\mathbb{G}\|_{\mathscr{L}(\mathcal{Y}_s,\mathcal{U}_s)}}\right).$$

In order to estimate $\epsilon_D^* := \|\mathbb{G}_S^* - (\mathbb{G}_{DS})^*\|_{\mathscr{L}(\mathcal{Y},\mathcal{U})}$, we recall the definition of $\mathbb{G}_m$ in (4.7) and of $\mathbb{G}_D$ in (4.8) and obtain

$$\begin{aligned}
\epsilon_D^* &\le \|\mathbb{P}_{\mathcal{U}}\|_{\mathscr{L}(\mathcal{U})}\|(\mathbb{G}_m)^* - (\mathbb{G}_D)^*\|_{\mathscr{L}(\mathcal{Y},\mathcal{U})}\|\mathbb{P}_{\mathcal{Y}}\|_{\mathscr{L}(\mathcal{Y})},\\
&\le \sqrt{T}(\int_0^T \|K_m(t)^* - \tilde{K}(t)^*\|^2_{\mathscr{L}(Y,U)}\,dt)^{1/2}.
\end{aligned} \tag{5.6}$$

We observe that

$$K_m(t) = P_U\kappa_U^{-1}\mathbf{K}(t)^*\kappa_Y P_Y \quad \text{and} \quad \tilde{K}(t)^* P_U\kappa_U^{-1}\tilde{\mathbf{K}}\kappa_Y P_Y \tag{5.7}$$

with $\mathbf{K}(t)^* = \mathbf{M}_U^{-1}\mathbf{K}(t)^T\mathbf{M}_Y$ and $\tilde{\mathbf{K}}(t)^* = \mathbf{M}_U^{-1}\tilde{\mathbf{K}}(t)^T\mathbf{M}_Y$, and that

$$\|\mathbf{K}(t)^* - \tilde{\mathbf{K}}(t)^*\|_{\mathbb{R}^{p,q}_w} = \|\mathbf{K}(t) - \tilde{\mathbf{K}}(t)\|_{\mathbb{R}^{q\times p}_w} \quad \text{for } t \in [0, T]. \tag{5.8}$$

Since each of the conditions in (5.2) ensures $\|\mathbf{K} - \tilde{\mathbf{K}}\|_{\mathbb{R}^{q\times p}_w} < \delta/2\sqrt{T}$, we have by means of (5.6) - (5.8) that $\epsilon_D^* < \delta/2$, which concludes the proof. $\square$

REMARK 13. *It remains to investigate the accuracy of the respective approximation of the (possibly regularized) pseudo-inverses* $(\mathbb{G}^*\mathbb{G} + \alpha\mathbb{I})^{-1}\mathbb{G}^*$ *with* $\alpha \ge 0$*, which play an important role e.g. in optimal control problems.*

6. Applications and numerical results.

6.1. Test problems. As test cases, we consider two heat equations on domains $\Omega \subset \mathbb{R}^2$ as depicted in Fig. 6.1 and with control and observation operators of the following form. Let $\Omega_c = (a_{c,1}, a_{c,2}) \times (b_{c,1}, b_{c,2})$ and $\Omega_m = (a_{m,1}, a_{m,2}) \times (b_{m,1}, b_{m,2})$ be rectangular subsets of Ω where the control is active and the observation takes place, respectively, with 4 appropriate points a_c, b_c, a_m, $b_m \in \bar{\Omega}$. Setting $U = Y = L^2(0,1)$, we define $C \in \mathscr{L}(L^2(\Omega), Y)$ and $B \in \mathscr{L}(U, L^2(\Omega))$ for test case 1 by

$$(Cz)(\xi) = \int_{a_{m,1}}^{b_{m,1}} \frac{z(x_1, x_2(\xi))}{b_{m,1} - a_{m,1}}\, dx_1, \quad (Bu)(x_1, x_2) = \begin{cases} u(\theta(x_1))\omega_c(x_2) & ,(x_1,x_2) \in \Omega_c \\ 0 & ,(x_1,x_2) \notin \Omega_c \end{cases},$$

where $\omega_c \in L^2(a_{c,2}, b_{c,2})$ is a weight function and $\theta : [a_{c,1}, b_{c,1}] \to [0,1]$ and $x_1 : [0,1] \to [a_{m,1}, b_{m,1}]$ are affine-linear transformations. For test case 2, we just invert the roles of x_1 and x_2 in the definition of C. Note that C preserves an inherent spatial state regularity, i.e. $C_{|H^2(\Omega)} \in \mathscr{L}(H^2(\Omega), H^2(0,1))$.

Test case 1. *We consider a heat equation with homogeneous Dirichlet boundary conditions on* $(0,T] \times \Omega$ *with* $T = 1$ *and* $\Omega = (0,1)^2$. *We choose* $\Omega_c = \Omega$, $\Omega_m = (0.1, 0.2) \times (0.1, 0.9)$ *and* $\omega_c(x_2) = \sin(\pi x_2)$. *In this case, the output to inputs of the special form* $u(t;\theta) = \sin(\omega_T \pi t)\sin(m\pi\theta)$ *with* $\omega_T, m \in \mathbb{N}$ *can be explicitely formulated in terms of the eigenfunctions of the Laplace operator.*

As test case 2, we consider two infinitely long plates of width 5 and height 0.2 which are connected by two rectangular bars as shown in the cross section in Fig. 6.1. We assume that the plates are surrounded by an insulating material and that we can heat the bottom plate and measure the temperature distribution in the upper plate.

Test case 2. *We consider a heat equation with homogeneous Neumann boundary conditions on* $(0,T] \times \Omega$ *with* $T = 1$ *and* Ω *as in Fig. 6.1, and choose* $\Omega_c = (0.05, 4.95) \times (0.05, 0.15)$, $\Omega_m = (0.05, 4.95) \times (0.85, 0.95)$ *and* $\omega_c(x_2) = \sin(\pi(x_2 - 0.05)/0.1)$.

The matrix approximations $\tilde{\mathbf{G}}$ of the i/o-maps $\mathbb{G}$ corresponding to the test cases have been calculated by means of a heat equation solver, which is based on the C++ FEM software library DEAL.II[5]. It realizes a discontinuous Galerkin scheme with adaptive space and time grids and applies goal-oriented DWR-based error control to ensure (4.9), see [35] for details.

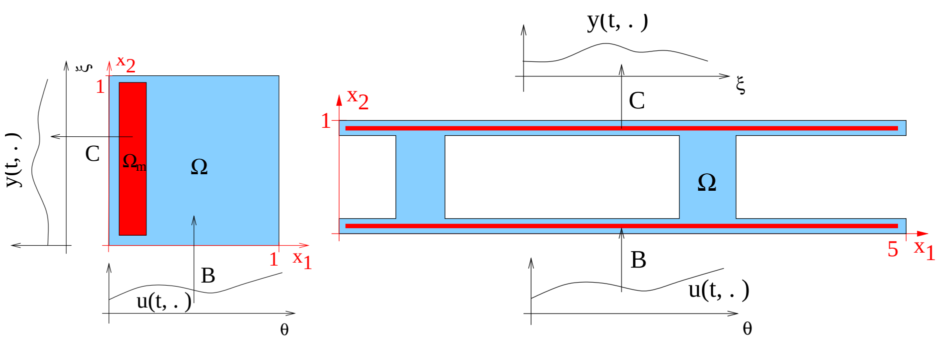

(a) Test case 1 (b) Test case 2

Fig. 6.1. *Test cases heat equation: (a) with homogeneous Dirichlet boundary conditions, (b) with homogeneous Neumann boundary conditions.*

6.2. Tests of convergence. The following numerical convergence tests have all been carried out with approximations $\mathbb{G}_{DS}(h_1, \tau_1, h_2, \tau_2, \texttt{tol})$ of the i/o-map $\mathbb{G}$ corresponding to Test case 1. Hierarchical linear finite elements in U_{h_1} and Y_{h_2} and Haar wavelets in $\mathcal{R}_{\tau_1}$ and $\mathcal{S}_{\tau_2}$ have been chosen. The tolerance `tol` refers to the estimate (4.11).

Convergence of single outputs. Considering Test case 1 with inputs $u(t;\theta) = \sin(\omega_T \pi t)\sin(m\pi\theta)$, and exactly known outputs $y = \mathbb{G}u$, we investigate the relative error $\|y - \tilde{y}\|_{\mathcal{Y}}/\|u\|_{\mathcal{U}_s}$, with $\tilde{y} = \mathbb{G}_{DS}(h_1, \tau_1, h_2, \tau_2, \texttt{tol})u$, for varying discretization parameters h_1, τ_1, h_2, τ_2 and `tol`. Choosing e.g. $m = 5$ and $\omega_T = 10$, we observe a quadratic convergence in $h_1 = h_2$ (cf. Fig. 6.2-a) and a linear convergence in $\tau_1 = \tau_2$ (cf. Fig. 6.2-b) in correspondence to Thm. 5.1. However, the error does not converge to zero but to a positive plateau value, which is due to the system dynamics error and which becomes smaller for lower tolerances `tol`. For input signals with $m > 5$ and $\omega_T > 10$ the convergence order can only be observed for smaller discretization parameters h_1, h_2, τ_1 and τ_2.

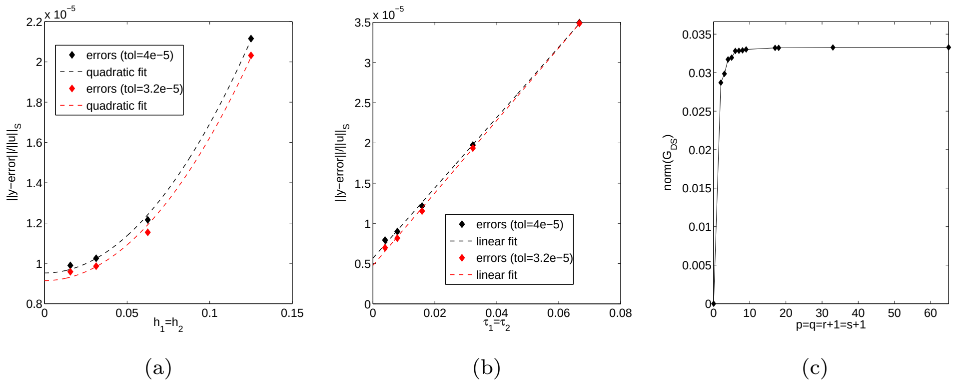

FIG. 6.2. *(a) Relative output errors for input $u(t;\theta) = \sin(10\pi t)\sin(5\pi\theta)$, varying $h_1 = h_2$ and fixed $\tau_1 = \tau_2 = 1/64$. (b) Relative output errors for input $u(t;\theta) = \sin(10\pi t)\sin(5\pi\theta)$, varying $\tau_1 = \tau_2$ and fixed $h_1 = h_2 = 1/17$. (c) Norm $\|\mathbb{G}_{DS}(\mathbf{h})\|_{\mathscr{L}(\mathcal{U},\mathcal{Y})}$ for synchronously increasing approximation space dimensions $p = q = r+1 = s+1$ and fixed tolerance* `tol` $= 4.0e-5$.

Convergence of the norm $\|\mathbb{G}_S(h_1, \tau_1, h_2, \tau_2)\|_{\mathscr{L}(\mathcal{U},\mathcal{Y})}$ for nested subspaces. Successively improving the signal approximation by adding additional basis functions, the norm $\|\mathbb{G}_S(h_1, \tau_1, h_2, \tau_2)\|_{\mathscr{L}(\mathcal{U},\mathcal{Y})}$ converges, cf. Lemma 3.1. We approximate $\|\mathbb{G}_S\|_{\mathscr{L}(\mathcal{U},\mathcal{Y})}$ by $\|\mathbb{G}_{DS}\|_{\mathscr{L}(\mathcal{U},\mathcal{Y})}$, where $\mathbb{G}_{DS}$ has been calculated with `tol` $= 4.0e-5$. In Fig. 6.2-c, the approximations $\|\mathbb{G}_S(h_1, \tau_1, h_2, \tau_2)\|_{\mathscr{L}(\mathcal{U},\mathcal{Y})} = \|\mathbb{G}_S(\frac{1}{p-1}, \frac{1}{r}, \frac{1}{q-1}, \frac{1}{s})\|_{\mathscr{L}(\mathcal{U},\mathcal{Y})}$ are plotted for increasing subspace dimensions $p = q = r+1 = s+1 = 2, 3, \ldots, 65$.

6.3. Matrix reduction on the basis of SVDs. In order to resolve the input and output signal spaces accurately by means of general purpose basis functions, a large number of basis functions is needed in general. In order to reduce the large size of the resulting i/o-matrices $\tilde{\mathbf{G}}$, we apply a reduction method known as *Tucker decomposition* or *higher order singular value decomposition* (HOSVD) [19]. It is based on singular value decompositions (SVDs) and preserves the space-time tensor structure of the input and output signal bases.

Considering $\tilde{\mathbf{G}} \in \mathbb{R}^{qs \times pr}$ as a fourth-order tensor $\tilde{\mathbf{G}} \in \mathbb{R}^{s \times r \times q \times p}$ with $\tilde{\mathbf{G}}_{ijkl} = \tilde{\mathbf{G}}_{ij}^{kl}$, it is shown in [19] that there exists a HOSVD

$$\tilde{\mathbf{G}} = \mathbf{S} \times_1 \mathbf{U}^{(\psi)} \times_2 \mathbf{U}^{(\phi)} \times_3 \mathbf{U}^{(\nu)} \times_4 \mathbf{U}^{(\mu)}. \tag{6.1}$$

Here $\mathbf{S} \in \mathbb{R}^{s\times r\times q\times p}$ is a so-called *core tensor*, satisfying some orthogonality properties, $\mathbf{U}^{(\psi)} \in \mathbb{R}^{s\times s}$, $\mathbf{U}^{(\phi)} \in \mathbb{R}^{r\times r}$, $\mathbf{U}^{(\nu)} \in \mathbb{R}^{q\times q}$, $\mathbf{U}^{(\mu)} \in \mathbb{R}^{p\times p}$ are unitary matrices and $\times_1, \ldots, \times_4$ denote tensor-matrix multiplications. We define a so-called *matrix unfolding* $\tilde{\mathbf{G}}^{(\psi)} \in \mathbb{R}^{s\times rqp}$ of the tensor $\tilde{\mathbf{G}}$ by

$$\tilde{\mathbf{G}}^{(\psi)}_{im} = \mathbf{G}_{ijkl}, \quad m = (k-1)ps + (l-1)s + i,$$

i.e. we put all elements belonging to $\psi_1, \psi_2, \ldots, \psi_s$ into one respective row, and we define the unfoldings $\tilde{\mathbf{G}}^{(\phi)} \in \mathbb{R}^{r\times qps}$, $\tilde{\mathbf{G}}^{(\nu)} \in \mathbb{R}^{q\times psr}$ and $\tilde{\mathbf{G}}^{(\mu)} \in \mathbb{R}^{p\times srq}$ in a similar cyclic way. Then, $\mathbf{U}^{(\psi)}$, $\mathbf{U}^{(\phi)}$, $\mathbf{U}^{(\nu)}$ and $\mathbf{U}^{(\mu)}$ in (6.1) can be calculated by means of four SVDs of the respective form

$$\tilde{\mathbf{G}}^{(\psi)} = \mathbf{U}^{(\psi)} \Sigma^{(\psi)} (\mathbf{V}^{(\psi)})^T,$$

where $\Sigma^{(\psi)}$ is diagonal with entries $\sigma_1^{(\psi)} \geq \sigma_2^{(\psi)} \geq \ldots \sigma_s^{(\psi)} \geq 0$ and $\mathbf{V}^{(\psi)}$ is columnwise orthonormal. The $\sigma_i^{(\psi)}$ are so-called *n-mode singular values* (or in our case ψ-mode singular values) of the tensor $\tilde{\mathbf{G}}$ and correspond to the Frobenius norms of certain subtensors of the core tensor $\mathbf{S}$.

On the basis of (6.1) we can define an approximation $\hat{\mathbf{G}} \in \mathbb{R}^{s\times r\times q\times p}$ of $\tilde{\mathbf{G}}$ by discarding the smallest n-mode singular values $\{\sigma^{(\psi)}_{\hat{s}+1}, \ldots, \sigma^{(\psi)}_s\}$, $\{\sigma^{(\phi)}_{\hat{r}+1}, \ldots, \sigma^{(\psi)}_r\}$, $\{\sigma^{(\nu)}_{\hat{q}+1}, \ldots, \sigma^{(\nu)}_q\}$ and $\{\sigma^{(\mu)}_{\hat{p}+1}, \ldots, \sigma^{(\mu)}_p\}$, i.e. we set the corresponding parts of $\mathbf{S}$ to zero. Then we have

$$\|\tilde{\mathbf{G}} - \hat{\mathbf{G}}\|_F^2 \leq \sum_{i=\hat{s}+1}^{s} \sigma_i^{(\psi)} + \sum_{j=\hat{r}+1}^{r} \sigma_j^{(\phi)} + \sum_{k=\hat{q}+1}^{q} \sigma_k^{(\nu)} + \sum_{l=\hat{p}+1}^{p} \sigma_l^{(\mu)},$$

see [19]. Note that, in contrast to matrix SVDs, this approximation is not necessarily optimal in a least square sense. For best-rank approximations, see e.g. [20].

The truncation of $\hat{\mathbf{G}} \in \mathbb{R}^{qr\times ps}$ after a basis transformation corresponding to $\mathbf{U}^{(\psi)}$, $\mathbf{U}^{(\phi)}$, $\mathbf{U}^{(\nu)}$ and $\mathbf{U}^{(\mu)}$ yields a low-dimensional representation $\bar{\mathbf{G}} \in \mathbb{R}^{\hat{q}\hat{r}\times\hat{p}\hat{s}}$.

In Figure 6.3 the HOSVD has been applied to a matrix $\tilde{\mathbf{G}} \in \mathbb{R}^{qs\times pr}$ for the Test case 2 with $p = 17$, $q = 65$ and $r = s = 64$. The first row shows the respective n-mode singular values. Underneath the first and most relevant two transformed/new basis functions $\hat{\mu}_i$, $\hat{\nu}_i$, $\hat{\phi}_i$ and $\hat{\psi}_i$, are plotted. It is not surprising that the positions of the connections between the plates can be recovered as large values of the corresponding spatial input and output basis functions.

Remark 14. *The application of a HOSVD can be useful in two ways.* First*, in order to obtain a low-dimensional matrix-representation of the system, which is small enough to be used for real-time feedback control design.* Second*, in order to identify relevant input and output signals, which may be instructive for actuator and sensor design, i.e. they might help to answer where actuators and sensors have to be placed and which resolution in time and space they should have.*

6.4. Application in optimization problems. We investigate the use of the i/o-map approximation in optimization problems

$$\min J(u, y) \qquad \text{subject to } y = \mathbb{G}u, \quad u \in \mathcal{U}_{ad}. \tag{6.2}$$

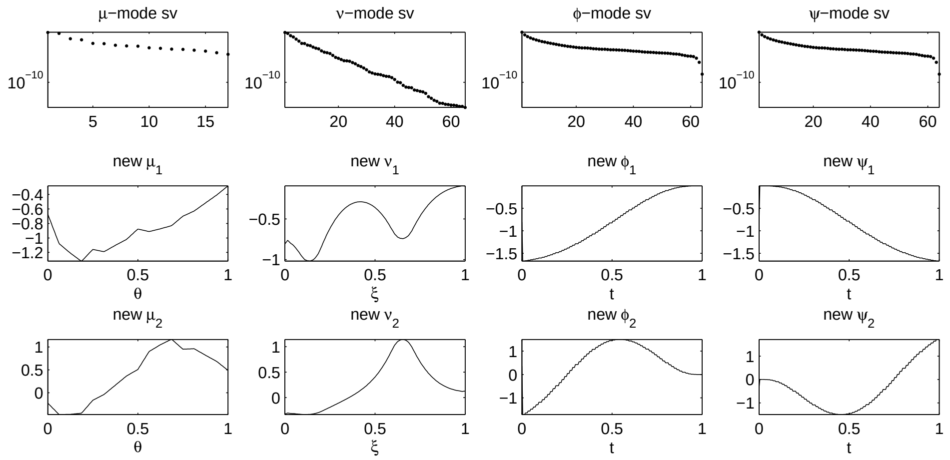

FIG. 6.3. *HOSVD applied to the i/o map of Test case 2. First row: n-mode singular values in semilogarithmic scales. 2nd and 3rd row: Respective two most relevant basis functions.*

Here $\mathcal{U}_{ad} \subset \mathcal{U}$ is the subset of admissible controls, $J : \mathcal{U} \times \mathcal{Y} \to \mathbb{R}$ is the quadratic cost functional $J(u, y) = \frac{1}{2}\|y - y_D\|^2_{\mathcal{Y}} + \alpha\|u\|^2_{\mathcal{U}}$, $y_D \in \mathcal{Y}$ is an aspired system's output signal, and $\alpha > 0$ is a regularization parameter. We define the discrete cost functional

$$\bar{J}_{\mathbf{h}} : \mathbb{R}^{pr} \times \mathbb{R}^{qs} \to \mathbb{R}, \qquad \bar{J}_{\mathbf{h}}(\mathbf{u}, \mathbf{y}) = \frac{1}{2}\|\mathbf{y} - \mathbf{y}_D\|^2_{qs;w} + \alpha\|\mathbf{u}\|^2_{pr;w}, \tag{6.3}$$

with $\mathbf{y}_D = \kappa_{\mathcal{Y},h_2,\tau_2}\mathbb{P}_{\mathcal{Y},h_2,\tau_2} y_D$, and instead of (6.2) we solve

$$\min \bar{J}_{\mathbf{h}}(\mathbf{u}, \mathbf{y}) \qquad \text{subject to } \mathbf{y} = \tilde{\mathbf{G}}\mathbf{u}, \quad \mathbf{u} \in \bar{U}_{ad} \tag{6.4}$$

with $\bar{U}_{ad} = \{\mathbf{u} \in \mathbb{R}^{pr} : \mathbf{u} = \kappa_{\mathcal{U},h_1,\tau_1}\mathbb{P}_{\mathcal{U},h_1,\tau_1} u,\ u \in \mathcal{U}_{ad}\}$. Considering optimization problems without control constraints, i.e. $\mathcal{U}_{ad} = \mathcal{U}$ and $\bar{U}_{ad} = \mathbb{R}^{pr}$, the solution $\bar{\mathbf{u}}$ of (6.4) is characterized by

$$(\tilde{\mathbf{G}}^T \mathbf{M}_{\mathcal{Y}} \tilde{\mathbf{G}} + \alpha \mathbf{M}_{\mathcal{U}})\bar{\mathbf{u}} = \tilde{\mathbf{G}}^T \mathbf{M}_{\mathcal{Y}} \mathbf{y}_D. \tag{6.5}$$

As concrete example, we consider Test case 2 and choose $y_D = \mathbb{G}u_0$ to be the output for an input $u_0 \equiv 1$ which is equal to 1 on all of $[0, T] \times (0, 1)$. We then try to find an *optimized* input u_* of less energy, such that $\mathbb{G}u_* \approx y_D$, or more exactly, u_* that minimizes the cost functional (6.2).

First we solve (6.5) with an approximated i/o map $\tilde{\mathbf{G}} \in \mathbb{R}^{17\cdot 64 \times 65\cdot 64}$ and $\alpha = 10^{-4}$, yielding an approximation $\bar{u} \approx u_*$. The solution takes 0.33 seconds on a normal desktop PC. The u-norm is reduced by 27.9% and the relative deviation of $\mathbb{G}\bar{u}$ from y_D is 9.4%. In Fig. 6.4 the same calculations have been carried out with $\hat{\mathbf{G}} \in \mathbb{R}^{3\cdot 5 \times 3\cdot 5}$, where $\hat{\mathbf{G}}$ arises from a HOSVD-based matrix reduction of $\tilde{\mathbf{G}} \in \mathbb{R}^{17\cdot 64 \times 65\cdot 64}$, where all but the 3 most relevant spatial and the 5 most relevant temporal input and output basis functions have been truncated. Using this approximation, the norm of u is reduced by 27.4%, whereas the relative deviation of $\mathbb{G}\bar{u}$ from y_D is 9.5%. The cost functional has been reduced by 44.5%, and the calculation of $\bar{u}$ took less than 0.0004 seconds. The outputs resulting from u_0 and $\bar{u}$ have been calculated in simulations independent from the calculation of the i/o-matrix.

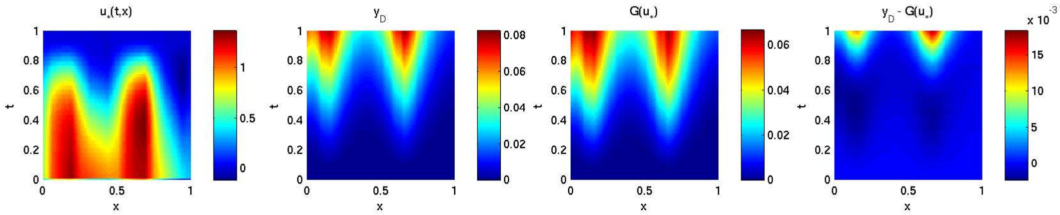

FIG. 6.4. *Application of the SVD-reduced approximated i/o map $\hat{\mathbf{G}} \in \mathbb{R}^{3\cdot 5\times 3\cdot 5}$ in an optimization problem. From left to right: optimized control $\bar{u}$, original output $y_D = \mathbb{G}u_0$, optimized output $\mathbb{G}\bar{u}$ and their difference.*

REMARK 15. *Aiming to realize the optimal control via a feedback control, we may look for feedback operators $\mathbb{F} \in \mathscr{L}(\mathcal{Y},\mathcal{U})$ satisfying $u_* = \mathbb{F}y_*$ for $y_* = \mathbb{G}u_*$. On the discrete level, we search for a matrix $\mathbf{F} \in \mathbb{R}^{pr\times qs}$ satisfying*

$$\bar{\mathbf{u}} = \mathbf{F}\bar{\mathbf{y}}, \quad \textit{where } \bar{\mathbf{y}} = \tilde{\mathbf{G}}\bar{\mathbf{u}} \tag{6.6}$$

and $\bar{\mathbf{u}}$ is the solution of (6.4). *We note that for $\bar{\mathbf{y}} \neq 0$, such a matrix $\mathbf{F}$ always exists. Requiring however, that $\mathbf{F}$ has extra structure like time-invariance and causality,* (6.6) *may only be solvable in a least square sense.*

7. Final remarks and outlook. We have presented a systematic framework for the discretization of i/o-maps of linear infinite-dimensional control systems with *spatially distributed* inputs and outputs. Global error estimates have been provided, which allow to choose the involved discretization parameters in such a way that a desired overall accuracy is achieved and that the signal and the system dynamics approximation errors are balanced. Moreover, the error results are capable to take many practical and technical restrictions in sensor and actuator design like limited spatial and temporal resolutions or the use of piece-wise constant controls and observations due to digital devices directly into account.

The numerical costs of the approach are primarily governed by the numerical calculation of p underlying homogeneous PDEs, where p is the number of input basis functions in space, which can become problematic when the spatial resolution of the input signal space has to be accurate. In this case, code-optimization, e.g. due to parallelization and appropriate updating of mass and stiffness matrices from prior calculations, promises to have a large potential for speed-up which has not yet been investigated.

The SVD-based dimension reduction for the matrix representation can be considered as an alternative model reduction approach, and the resulting reduced i/o-models prove to be useful in first numerical optimization applications. Moreover, the SVD-based reduction may be able to provide useful insight for efficient actuator and sensor design by filtering out relevant input and output signals.

Acknowledgement. The author would like to thank Christian Kamm for his assistance in the development of the heat equation solver with DWR error estimation.

REFERENCES

[1] M. Ainsworth and J. T. Oden. *A posteriori error estimation in finite element analysis.* Pure and Applied Mathematics (New York). Wiley-Interscience, New York, 2000.

[2] A. C. Antoulas. Frequency domain representation and singular value decomposition. *UNESCO EOLSS*, Contribution 6.43.13.4, 2001.

[3] A. C. Antoulas. *Approximation of large-scale dynamical systems*, volume 6 of *Advances in Design and Control*. Society for Industrial and Applied Mathematics (SIAM), Philadelphia, PA, 2005.

[4] I. Babuska and A. Miller. The post-processing approach in the finite element method. III. A posteriori error estimates and adaptive mesh selection. *Int. J. Numer. Methods Eng.*, 20:2311–2324, 1984.

[5] W. Bangerth, R. Hartmann, and G. Kanschat. `deal.II` *Differential Equations Analysis Library, Technical Reference*. http://www.dealii.org/, 5.2 edition, sept 2005.

[6] W. Bangerth and R. Rannacher. *Adaptive finite element methods for differential equations*. Lectures in Mathematics ETH Zürich. Birkhäuser, Basel, 2003.

[7] R. Becker, M. Garwon, C. Gutknecht, G. Bärwolff, and R. King. Robust control of separated shear flows in simulation and experiment. *Journal of Process Control*, 15:691–700, 2005.

[8] R. Becker, V. Heuveline, and R. Rannacher. An optimal control approach to adaptivity in computational fluid mechanics. *Int. J. Numer. Methods Fluids*, 40(1-2):105–120, 2002.

[9] R. Becker and R. Rannacher. A feed-back approach to error control in finite element methods: basic analysis and examples. *East-West J. Numer. Math.*, 4(4):237–264, 1996.

[10] R. Becker and R. Rannacher. An optimal control approach to a posteriori error estimation in finite element methods. *Acta Numer.*, 10:1–102, 2001.

[11] R. Becker and R. Rannacher. Error control for model reduction by discretization in optimal control of flows. In *Topics in mathematical fluid mechanics*, volume 10 of *Quad. Mat.*, pages 33–59. Dept. Math., Seconda Univ. Napoli, Caserta, 2002.

[12] P. Benner, V. Mehrmann, and D. Sorensen (Editors). *Dimension Reduction of Large-Scale Systems*, volume 45 of *LNSCE*. Springer, Heidelberg, 2005.

[13] P. Benner, V. Mehrmann, V. Sima, S. Van Huffel, and A. Varga. SLICOT—a subroutine library in systems and control theory. In *Applied and computational control, signals, and circuits, Vol. 1*, volume 1 of *Appl. Comput. Control Signals Circuits*, pages 499–539. Birkhäuser Boston, Boston, MA, 1999.

[14] G. Berkooz, P. Holmes, and J. L. Lumley. The proper orthogonal decomposition in the analysis of turbulent flows. In *Annual review of fluid mechanics, Vol. 25*, pages 539–575. Annual Reviews, Palo Alto, CA, 1993.

[15] M. Braack and A. Ern. A posteriori control of modeling errors and discretization errors. *Multiscale Model. Simul.*, 1(2):221–238 (electronic), 2003.

[16] P. G. Ciarlet. *The finite element method for elliptic problems*, volume 40 of *Classics in Applied Mathematics*. Society for Industrial and Applied Mathematics (SIAM), Philadelphia, PA, 2002.

[17] A. Cohen. *Numerical analysis of wavelet methods*, volume 32 of *Studies in Mathematics and its Applications*. North-Holland Publishing Co., Amsterdam, 2003.

[18] R. F. Curtain. Model reduction for control design for distributed parameter systems. In *Research directions in distributed parameter systems (Raleigh, NC, 2000)*, volume 27 of *Frontiers Appl. Math.*, pages 95–121. SIAM, Philadelphia, PA, 2003.

[19] L. De Lathauwer, B. De Moor, and J. Vandewalle. A multilinear singular value decomposition. *SIAM J. Matrix Anal. Appl.*, 21(4):1253–1278, 2000.

[20] L. De Lathauwer, B. De Moor, and J. Vandewalle. On the best rank-1 and rank-$(R_1, R_2, \cdots, R_N)$ approximation of higher-order tensors. *SIAM J. Matrix Anal. Appl.*, 21(4):1324–1342, 2000.

[21] B. De Schutter. Minimal state-space realization in linear system theory: an overview. *J. Comput. Appl. Math.*, 121(1-2):331–354, 2000.

[22] E. Emmrich. *Gewöhnliche und Operator-Differentialgleichungen*. Vieweg, Wiesbaden, 2004.

[23] K. Eriksson, D. Estep, P. Hansbo, and C. Johnson. Introduction to adaptive methods for differential equations. In *Acta numerica, 1995*, Acta Numer., pages 105–158. Cambridge Univ. Press, Cambridge, 1995.

[24] K. Eriksson and C. Johnson. Adaptive finite element methods for parabolic problems. II. Optimal error estimates in $L_\infty L_2$ and $L_\infty L_\infty$. *SIAM J. Numer. Anal.*, 32(3):706–740, 1995.

[25] L. C. Evans. *Partial differential equations*, volume 19 of *Graduate Studies in Mathematics*. American Mathematical Society, Providence, RI, 1998.

[26] R. W. Freund. Model reduction methods based on Krylov subspaces. Technical report, Bell Laboratories, Lucent Technologies, 2001.

[27] J. Gerhard, M. Pastoor, R. King, B.R. Noack, A. Dillmann, M. Morzynski, and G. Tadmor. Model-based control of vortex shedding using low-dimensional galerkin models. *AIAA-*

Paper 2003-4262, 2003.
[28] S. Gugercin and A. C. Antoulas. A survey of model reduction by balanced truncation and some new results. *Internat. J. Control*, 77(8):748–766, 2004.
[29] W. Hackbusch, B. N. Khoromskij, and E. E. Tyrtyshnikov. Hierarchical Kronecker tensor-product approximations. *J. Numer. Math.*, 13(2):119–156, 2005.
[30] L. Henning, D. Kuzmin, V. Mehrmann, M. Schmidt, A. Sokolov, and S. Turek. Flow control on the basis of a featflow-matlab coupling. *Appears in: Active Flow Control 2006, Berlin, Germany, September 27 to 29, 2006. Berlin: Springer. Notes on Numerical Fluid Mechanics and Multidisciplinary Design (NNFM)*, 2006.
[31] V. Heuveline and R. Rannacher. Duality-based adaptivity in the *hp*-finite element method. *J. Numer. Math.*, 11(2):95–113, 2003.
[32] C. Johnson. *Numerical solution of partial differential equations by the finite element method.* Cambridge University Press, Cambridge, 1987.
[33] C. Johnson and R. Rannacher. On errror control in CFD. In *Hebeker, Friedrich-Karl (ed.) et al., Numerical methods for the Navier-Stokes equations. Proceedings of the international workshop held, Heidelberg, Germany, October 25-28, 1993. Notes Numer. Fluid Mech. 47, 133-144* . Vieweg, Braunschweig, 1994.
[34] C. Johnson, R. Rannacher, and M. Boman. Numerics and hydrodynamic stability: toward error control in computational fluid dynamics. *SIAM J. Numer. Anal.*, 32(4):1058–1079, 1995.
[35] C. Kamm and M. Schmidt. Dual-weighted residual error estimation for the heat equation in practice. Technical report, TU Berlin, Institute of Mathematics, in preparation, 2006.
[36] O. Lehmann, D.M. Luchtenburg, B.R. Noack, R. King, M. Morzynski, and G. Tadmor. Wake stabilization using pod galerkin models with interpolated modes. In *Proceedings of the 44th IEEE Conference on Decision and Control and European Conference ECC, Invited Paper 1618*, 2005.
[37] J.-L. Lions and E. Magenes. *Non-homogeneous boundary value problems and applications. Vol. II.* Springer, New York, 1972.
[38] A. Lunardi. *Analytic semigroups and optimal regularity in parabolic problems.* Progress in Nonlinear Differential Equations and their Applications, 16. Birkhäuser, Basel, 1995.
[39] The MathWorks, Inc., Cochituate Place, 24 Prime Park Way, Natick, Mass, 01760. Matlab Version 7.0.4.352 (R14), 2005.
[40] M. Pastoor, R. King, B.R. Noack, A. Dillmann, and G. Tadmor. Model-based coherent-structure control of turbulent shear ows using low-dimensional vortex models. *AIAA-Paper 2003-4261*, 2003.
[41] A. Pazy. *Semigroups of linear operators and applications to partial differential equations*, volume 44 of *Applied Mathematical Sciences*. Springer, New York, 1983.
[42] C. W. Rowley. Model reduction for fluids, using balanced proper orthogonal decomposition. *Internat. J. Bifur. Chaos Appl. Sci. Engrg.*, 15(3):997–1013, 2005.
[43] Clarence W. Rowley, Tim Colonius, and Richard M. Murray. Model reduction for compressible flows using POD and Galerkin projection. *Phys. D*, 189(1-2):115–129, 2004.
[44] H. Sohr. *The Navier-Stokes equations.* Birkhäuser Advanced Texts: Basler Lehrbücher. Birkhäuser, Basel, 2001.
[45] V. Thomée. *Galerkin finite element methods for parabolic problems*, volume 25 of *Springer Series in Computational Mathematics*. Springer, Berlin, 1997.
[46] F. Tröltzsch. *Optimale Steuerung partieller Differentialgleichungen*. Vieweg, Wiesbaden, 2005.
[47] D. Werner. *Funktionalanalysis*. Springer, Berlin, extended edition, 2000.
[48] K. Willcox and J. Peraire. Balanced model reduction via the proper orthogonal decomposition. *AIAA Journal*, 2002.
[49] H. Yserentant. Hierarchical bases in the numerical solution of parabolic problems. In *Large scale scientific computing (Oberwolfach, 1985)*, volume 7 of *Progr. Sci. Comput.*, pages 22–36. Birkhäuser Boston, Boston, MA, 1987.
[50] H. Yserentant. Hierarchical bases. In *ICIAM 91 (Washington, DC, 1991)*, pages 256–276. SIAM, Philadelphia, PA, 1992.
[51] E. Zeidler. *Nonlinear functional analysis and its applications. II/A*. Springer, New York, 1990.